

UCSF

UC San Francisco Electronic Theses and Dissertations

Title

Suppression of the DNA damage checkpoint by the *Saccharomyces cerevisiae* polo-like kinase, CDC5, to promote adaptation

Permalink

<https://escholarship.org/uc/item/88c9w6n9>

Author

Vidanes, Genevieve Medina

Publication Date

2009

Peer reviewed|Thesis/dissertation

Suppression of the DNA damage checkpoint by the *Saccharomyces cerevisiae*

polo-like kinase, *CDC5*, to promote adaptation

by Genevieve M. Vidanes

DISSERTATION

Submitted in partial satisfaction of the requirements for the degree of

DOCTOR OF PHILOSOPHY

in

Cell Biology

in the

GRADUATE DIVISION

of the

UNIVERSITY OF CALIFORNIA, SAN FRANCISCO

Copyright 2009

by

Genevieve M. Vidanes

Acknowledgements

Portions of this work have been published elsewhere. Chapter 1 was previously published in *Trends in Biochemical Sciences*, 2005 February, volume 30, number 2, Garber PM, Vidanes GM, and Toczyski DP, Damage in Transition, pages 63-66. Chapter 2 was previously published in *Cell*, 2005 July, volume 121, number 7, Vidanes G, Bonilla C, and Toczyski D, Complicated Tails: Histone Modifications and the DNA Damage Response, pages 973-976.

The contents of Chapter 4 have been submitted for publication elsewhere. FD Sweeney and S Galicia performed the *in vitro* Cdc5 kinase assays in Figures 4C, 4D, and Supplemental Figure 3.

Unless otherwise specified above, the work presented in this dissertation was performed by Genevieve M. Vidanes, under the direction and supervision of David P. Toczyski.

**Suppression of the DNA damage checkpoint by the
Saccharomyces cerevisiae polo-like kinase, *CDC5*,
to promote adaptation**

by

Genevieve M. Vidanes

Abstract

To counter the threat of genomic damage, an evolutionarily conserved checkpoint system exists that recognizes the presence of damaged DNA, prevents cell cycle progression, and promotes repair. We were interested in understanding the mechanisms of (I) checkpoint initiation and (II) checkpoint termination during adaptation in *Saccharomyces cerevisiae*. The 9-1-1 clamp is a checkpoint sensor that is recruited to double-strand breaks (DSBs). Regarding checkpoint initiation, we examined the both the generic requirements and the recruitment patterns of the 9-1-1 checkpoint clamp to an engineered DSB. We discovered that while the 9-1-1 clamp shares structural and mechanical similarities with the PCNA-replication clamp to associate with DNA at ssDNA/dsDNA junctions, the genetic requirements for *in vivo* recruitment varied. Both clamp structures required the single-stranded binding protein complex, RPA. However, the 9-1-1 complex did not utilize the replication Pol α -primase complex, which creates the ssDNA/dsDNA junctions recognized by PCNA. These data suggested the functional difference between the checkpoint and replication clamps lies in the substrate specificity. Regarding our interest in adaptation, we determined how the Cdc5 polo-like kinase acts to promote adaptation. Adaptation is a survival mechanism, in which yeast cells will escape a checkpoint arrest if DNA damage has not been repaired after several hours, and has been previously shown to require Cdc5. The overexpression of Cdc5 was used as a tool to probe how Cdc5 impacts checkpoint signaling. We found that Cdc5 overproduction had no significant effect on initial steps of checkpoint signaling, including recruitment of checkpoint sensors to damage and activity of initiating checkpoint kinases. However, the downstream checkpoint-effector kinase, Rad53, lost its

damage-dependent hyperphosphorylation, suggesting Cdc5 may inhibit the amplification step of the checkpoint-signaling cascade.

Table of Contents

CHAPTER 1: Damage in Transition.....	1
CHAPTER 2: Complicated Tails: Histone Modifications and the DNA Damage Response.....	10
CHAPTER 3: Calling 9-1-1: Recruitment of the 9-1-1 Complex to DNA Damage.....	24
CHAPTER 4: Learning to adapt: Suppression of the DNA Damage Checkpoint by the <i>Saccharomyces cerevisiae</i> Polo-like Kinase, CDC5, to Promote Adaptation.....	43
APPENDIX.....	75
BIBLIOGRAPHY.....	79

List of Tables and Figures

CHAPTER 1

Figure 1. Model of DSB repair: NHEJ vs. HR.....8

CHAPTER 2

Figure 1. Models of recruitment to a DSB via histone modification.....22

CHAPTER 3

Figure 1. RPA co-localizes to DSBs and is required for checkpoint localization.....38

Figure 2. Pol α -primase displays cell-cycle dependent and DNA-damage independent localization patterns.....39

Figure 3. RPA but not Pol α -primase mutants display checkpoint defects.....40

Figure 4. Distal spreading of RPA, Ddc1, and Ddc2 from an HO break.....41

Figure 5. Ddc1 localization coincides with ssDNA proximal to a DSB.....42

CHAPTER 4

Figure 1. *CDC5* overexpression promotes adaptation by suppressing checkpoint signaling.....66

Figure 2. *CDC5* impinges on checkpoint signaling pathway at the step of Rad53 phosphorylation.....68

Figure 3. Suppression of Rad53 phosphorylation requires Cdc5 kinase activity but is independent of Ptc2, Ptc3, or Cdc14 phosphatases.....69

Figure 4. Rad53 interacts with and is phosphorylated by Cdc5 *in vivo* and *in vitro*.....71
Supplemental Figure 1. Rad9-Rad9 interaction unaffected by Cdc5.....73
Supplemental Figure 2. Cdc5 and Rad53 interact *in vivo* independently of damage.....74
Supplemental Figure 3. Cdc5 phosphorylates Rad53 *in vitro*.....74
Supplemental Figure 4. rad53-R70A hyperphosphorylation is suppressed by Cdc5.....74

APPENDIX

Table 1. Yeast strain collection.....76

Chapter 1

Damage in transition: Choosing between
Non-homologous End Joining and Homologous Recombination

ABSTRACT.

Double-stranded DNA breaks (DSBs) are a particularly dangerous form of DNA damage, as they can lead to chromosome loss, translocations, or truncations. When a DSB occurs, many proteins are recruited to the break site. These proteins serve to both initiate DNA repair and to activate a checkpoint response. Repair occurs through one of two pathways: nonhomologous end-joining (NHEJ), in which broken DNA ends are directly ligated; or homologous recombination (HR), in which a homologous chromosome is utilized as a template in a replicative repair process. The checkpoint response is mediated by the PI3K-like kinases, Mec1 and Tel1 (ATR and ATM in humans, respectively). Two recent studies in yeast have significantly increased our understanding of when each of the proteins involved in these processes is localized to a break, as well as how their sequential localization is achieved. Specifically, these studies support and expand upon a model in which Tel1 and the NHEJ proteins are the first proteins to localize to the break in order to initiate signaling and attempt repair, but are subsequently replaced by Mec1 and the HR proteins. This transition is mediated by a Cdk-dependent initiation of 5' to 3' processing (resection) of the DSB. Thus, the cell cycle stage at which DSBs occur affects the way in which the DSBs are processed and recognized.

The checkpoint proteins. The DNA damage checkpoint is comprised of at least two damage-recognition complexes: the PCNA-like 9-1-1 complex and one of two PI3 kinase-related protein kinases [1]. The 9-1-1 complex is loaded at damage sites by a replication factor C variant containing Rad24 [2,3] in a manner dependent upon the

heterotrimeric, single-stranded DNA (ssDNA) binding protein RPA [4]. One of the PI3K-like kinases, Mec1 is also thought to recognize ssDNA through RPA [5], an interaction that likely occurs through its associated subunit Ddc2 (ATRIP in humans) [5]. In contrast, the PI3K-like protein kinase Tel1 appears to bind DSBs through a complex of three proteins: Mre11, Rad50, and Xrs2, called the MRX complex (MRN in humans) [6].

The repair proteins. In addition to its role in recruitment of Tel1 to damage sites, the MRX complex promotes the ligation of broken DNA during NHEJ. The exact role of the MRX complex in NHEJ is not understood, although the MRX complex has several activities associated with it, including both endo and exonucleolytic activities, Tel1 targeting, telomere maintenance, and DNA binding [7]. The MRX complex works in conjunction with Ku and other proteins to promote DNA ligase IV-mediated joining of broken ends [8].

HR is carried out by the sequential function of several proteins, including Rad52, Rad51, Rad54 and RPA [9]. In current models, RPA binds a 3' ssDNA overhang, thus eliminating secondary structure. Next, Rad51 is loaded onto the ssDNA in a Rad52 dependent manner, thus displacing RPA. Subsequently, other recombinases, such as the Rad55/Rad57 complex and the chromatin remodeling protein Rad54, bind to help promote synapsis [9,10,11].

Processing of double-stranded DNA breaks. DNA damage can take myriad forms. Over the last 15 years, it has been suggested that many signaling events that occur in response to DNA damage actually do so by recognizing ssDNA generated as a

consequence of damage. DSBs are no exception. DSBs can be induced by exogenous sources, such as gamma irradiation, or endogenously, such as when a template containing a single-stranded nick is replicated. After a 1-2 hour lag, DSBs are subjected to 5' to 3' exonucleolytic degradation, a process referred to as resection, [12]. This processing is a prerequisite for homologous recombination and can be extensive (up to many thousands of bases) [13]. In contrast, NHEJ-mediated repair of an enzymatically generated DSB in yeast is normally religated with no loss of information, and likely no processing. However, in most mammalian cells (and in yeast in some circumstances) DSBs are processed to uncover regions of homology prior to NHEJ.

While resection is clearly required for HR, its regulation and mechanisms are not well understood [8]. Exo1, a single-stranded exonuclease, is important for resection in some contexts. However, significant processing still occurs when *EXO1* is deleted. The MRX complex can also promote resection. This function of the MRX complex was discovered through an allele of *RAD50*, called *RAD50S*, that eliminates processing of DSBs in meiosis. One component of the MRX complex, Mre11, has exonuclease activity *in vitro*, but this activity is not in the direction that one would expect for an exonuclease that mediates resection (it is a 3' to 5' exonuclease). Another gene required for meiotic DSB processing is *SAE2*. Interestingly, either deletion of *SAE2* or the *RAD50S* allele strongly amplifies Tel1's normally modest role in the DNA damage checkpoint. This result suggests that Tel1's ability to signal at a DSB is disrupted by processing of the DSB.

Ordered recruitment of proteins to a DSB. A new study from the Rothstein laboratory provides a comprehensive analysis of the localization of all of the aforementioned yeast proteins to sites of DNA damage [14]. By examining individual cells through time, and visualizing multiple damage-responsive proteins simultaneously, they determined the order in which proteins arrive at damage sites. Unlike early studies using formaldehyde-mediated chromatin immunoprecipitation (ChIP), which averages the population, direct visualization of multiple proteins at the same time allowed the Rothstein lab to determine which associations occurred simultaneously at a single break and which were mutually exclusive. These data showed directly that the MRX complex, and thus Tel1, localize to DSBs almost immediately after damage. Concurrently or shortly thereafter, the Sae2 protein arrives, and the MRX and Tel1 proteins are lost (Fig. 1, step a). Deletion of the *SAE2* gene (or the presence of the *RAD50S* allele) delays loss of the MRX protein Mre11, suggesting a causal role for Sae2 in this event. Consistent with the notion that the localization of Sae2 corresponds to the initiation of resection, RPA arrives at roughly the same time, as do the Mec1/Ddc2 and 9-1-1 complexes, both of which require RPA for their loading (Fig. 1, step d). Like Mec1/Ddc2 and the 9-1-1 complex, the recombinases make their appearance only after the MRX and Tel1 complexes have left. Interestingly, Lisby *et al.* show that Rad52 foci form in the absence of any of the tested recombinases, including Rad51 and the Swi2/Snf2 protein Rad54 (Fig. 1, steps e-f). In contrast, previously published data showed that Rad52's ability to ChIP DNA adjacent to DSBs is dramatically decreased in Rad51 and Rad54 mutants [10]. While these differences may reflect a difference in the methods used (e.g. DSB induction using the HO endonuclease vs irradiation), it could also reflect the fact that these experiments are asking subtly

different questions. Focus formation indicates that Rad52 has been targeted to the break, whereas ChIP additionally requires Rad52 to associate with DNA in such a way that it can be crosslinked. Taken together these data suggest that different modes of Rad52 association could be distinguished by these mechanisms.

Cdk regulation of the transition. At the heart of the transition from NHEJ to HR, or from Tel1 to Mec1/Ddc2, is the initiation of processing of a DSB [12]. Ira *et al.* have now linked the regulation of this transition to cell cycle position, or more specifically, to Cdk activity (Fig. 1, steps b-c) [15]. While previous reports had suggested that some resection can occur in G1, this study used a chemically inhibitable allele of *CDC28*, *cdc28-as1*, that allowed its authors to completely inhibit Cdc28 activity [16]. These experiments showed Cdc28 activity is required to initiate resection [15]. Consistently, RPA, Rad51 and Mec1/Ddc2 are not recruited to a DSB in G1, whereas the MRX complex is. To examine the effect of eliminating resection on checkpoint activation, Ira *et al.* monitored Rad53 phosphorylation, a downstream target of the checkpoint pathway. When cells are blocked in G1, Rad53 is not phosphorylated in response to a DSB. However, Rad53 is strongly phosphorylated in G1 in response to the UV-mimetic drug 4NQO, which generates ssDNA through a Cdk-independent mechanism. The fact that MRX recruitment, and presumably Tel1 recruitment, does not lead to Rad53 activation suggests that other vital checkpoint factors are unable to load in sufficient quantity in the absence of resection to effect checkpoint activation after a single DSB. In contrast, in response to other forms of damage, the MRX complex and Tel1 can facilitate Rad53 phosphorylation when processing is delayed by deletion of *SAE2* [17]. It should be noted

that Tel1 and Mec1/Ddc2 have substrates outside of the checkpoint pathway, such as H2A (equivalent to the H2AX phosphorylation in mammalian cells). In a related manuscript, Tel1 has been shown to be responsible for H2A phosphorylation in G1 arrested, and thus unresected, cells [18].

The NHEJ/HR choice in mammalian cells. While in yeast the vast majority of DSBs are repaired by HR [19], in mammals, NHEJ and HR play roughly equivalent roles [20]. Viewed in terms of the 'handoff' model outlined above, this difference might be explained by slower initiation of end resection in mammalian cells. This would allow the MRN-ATM complex to persist at the break site, increasing the time available for successful NHEJ to occur. Consistent with this model, checkpoint defects associated with *ATM* deficiency in mammals are severe [21], while the checkpoint defects of yeast *tel1* mutants are subtle [17].

An important difference between yeast and vertebrates that may be relevant to the NHEJ/HR choice is that vertebrates have evolved an additional PI3K-like protein kinase that acts in the DSB-response pathway. This kinase, called DNA-dependent protein kinase (DNA-PK), is required for NHEJ, associates with Ku and is activated by binding to DSBs. Intriguingly, DNA-PK mutants have a defect in DSB repair that is suppressed by further mutation of Ku [22]. Thus, in mammals, Ku appears to block HR, and channel breaks into the NHEJ pathway in a DNA-PK-dependent manner. Furthermore, DNA-PK may contribute to cell-cycle regulation of the NHEJ/HR choice, since its phosphorylation, kinase activity, and ability to form foci are all higher in G1

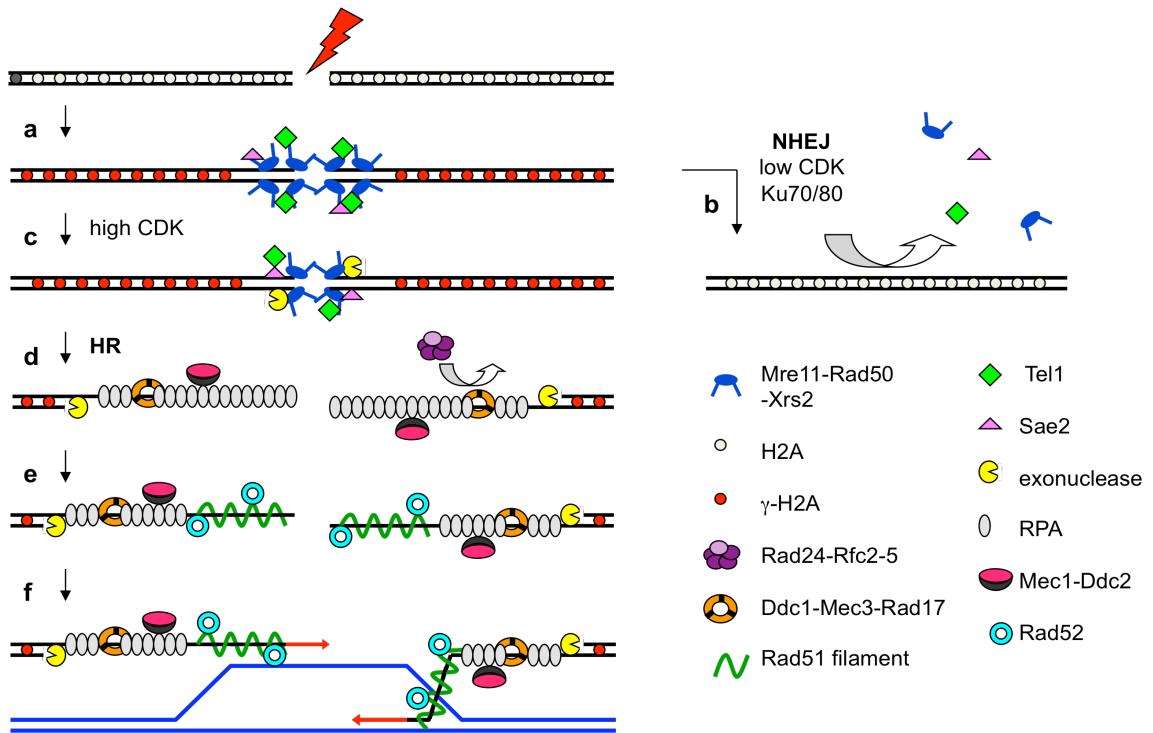
than in S-G2 [23]. Thus, in mammalian cells, DNA-PK appears to contribute to regulation of the HR-NHEJ choice in a way not available to yeast.

Despite these differences, many other features of the DSB response appear to be conserved between yeast and mammals. As in yeast, mammalian MRN components are among the first proteins to arrive at sites of damage [24], and their presence has been shown in some studies to be mutually exclusive with that of HR proteins [25]. Furthermore, genetic and biochemical studies indicate that MRN and ATM function in a common checkpoint/repair pathway [1]. Moreover, mammalian cells, like yeast cells, are more likely to repair DSB's by NHEJ in G1 and by HR in G2-M [26]. Thus, the broad outline of break repair described by these studies in yeast, wherein the MRN complex plays a primary role in sensing DSBs, and channels the break into either NHEJ or HR in a process that is influenced by cell-cycle position, is likely conserved in mammalian cells.

Figure Legends

Figure 1. Model of DSB Repair: NHEJ vs. HR. (a) Initial formation of a double-strand break recruits the early checkpoint components: Mre11-Rad50-Xrs2 complex, Tel1, and Sae2. Phosphorylation of histone H2A (g-H2A) quickly spreads distally from the break. (b) NHEJ, via Ku70 and Ku80, is an early repair pathway that is preferred when CDK activity is low. (c) When CDK activity is high, resection at the break occurs and MRX, Tel1 and Sae2 begin to dissociate. (d) RPA binds the exposed ssDNA and recruits Ddc2-

Mec1 while Rad24-Rfc2-5 deposits Ddc1-Mec3-Rad17 at the break site. (e-f) Rad52 and Rad51 are recruited to the break, displace RPA, and initiate strand invasion for HR.



Chapter 2

Complicated Tails: Histone Modifications and
the DNA damage response.

Abstract

In recent years, several ATP-dependent chromatin remodeling complexes and covalent histone modifications have been implicated in the response to double-stranded DNA breaks (DSBs). When a DSB occurs, cells must identify the DSB, activate the DNA damage checkpoint, and repair the break. Chromatin modification appears to be important, but not essential, for both of these processes, yet its precise mechanistic roles are only beginning to come into focus. Here, we discuss the role of chromatin in signaling by the DNA damage checkpoint pathway.

Introduction

On induction of a DSB, the 5' strand of DNA is selectively degraded at a rate of 3-4 kb/hr. This process, called resection, is a required processing step for some forms of DNA repair, such as homologous recombination and single-strand annealing. Both of these repair pathways are homology-based, and production of a single-stranded DNA (ssDNA) end aids in the identification of complementary sequences. Resection also serves to effectively amplify the signal emanating from a single DSB, as many checkpoint proteins are thought to recognize the ssDNA. The data discussed here suggest that the chromatin adjacent to this ssDNA may also have a role in repair and signaling.

Three classes of proteins are thought to initiate damage checkpoint signaling: two related PI3K-like kinases called ATR and ATM; a PCNA-like heterotrimeric ring, called the 9-1-1 complex; and a loosely defined set of adapter proteins, many of which contain BRCT domains [1]. This last class is represented by the archetypal *S. cerevisiae* checkpoint protein Rad9, and two quite divergent proteins, *S. pombe* Crb2 and human

53BP1. While we will treat these three proteins as homologs here, it should be noted that they do not have extensive sequence similarity nor do they function identically in yeast and man. These adapter proteins are thought to promote the phosphorylation/activation of downstream serine/threonine kinases, such as scRad53, hChk2, and spChk1.

Studies have indicated that each of the first two classes, ATR/ATM and the 9-1-1 complex, localize to sites of damage independently [1]. ATM, called Tel1 in *S. cerevisiae* and *S. pombe*, associates with DNA damage through the MRN complex (composed of Mre11, Rad50, and Nbs1), which also has an independent role in DNA repair. ATR is thought to subsequently associate, indirectly, with the ssDNA uncovered by resection. Loading of the 9-1-1 complex is less well understood, although it has been suggested that it occurs at ssDNA/dsDNA junctions, such as at the resecting 5' strand. Here, we will review data suggesting that both phosphorylation and methylation of histones help target the adaptor protein Rad9/Crb2/53BP1 to DSBs.

H2AX phosphorylation

Eukaryotic DNA is wrapped in a complex of eight histone molecules, generating a structure called the nucleosome. Every nucleosome contains two copies each of four histones: H2A, H2B, H3, and H4. In addition, several variant forms of histones exist. For H2A, these include H2AX, H2AZ, MacroH2A, and H2A-Bbd [27]. H2AX makes up a considerable portion of the H2A pool, ~2-25% in mammals. Phosphorylation of the C-terminus of H2AX is an evolutionarily conserved response to DSBs (Table 1). In humans, the H2AX C-terminal tail is a short extension beyond a conserved core region that distinguishes this variant from the canonical H2A1 histone. Although the length of

the tail can vary in different species, the four amino acids from the C-terminus of H2AX are highly conserved. Most importantly, the SQ residues at the -4 and -3 positions from the C terminus (which represent the ATR/ATM consensus site) are invariant. Although both *S. cerevisiae* and *S. pombe* lack a separate H2AX variant, the H2A histones that make up ~90% of the H2A pool carry an analogous C-terminal serine, and this site is also phosphorylated upon DNA damage. Phosphorylated mammalian H2AX and yeast H2A will both be referred to as γ -H2AX. This phosphorylation is thought to be carried out by Tel1/Mec1 and ATM/ATR in yeast and metazoans, respectively, although metazoan H2AX may also be targeted by the related PI3K-like kinase DNA-PK [28].

Phosphorylation of H2AX is one of the earliest responses to DNA damage. Within minutes of ionizing radiation (IR), γ -H2AX foci have been observed by immunofluorescence in mammalian cells [28,29,30]. These damage-induced foci have been demonstrated to form at double-strand breaks and increase in size over time. Laser scissors, which induce DSBs along the path of a laser across cells, induce a coincident pattern of γ -H2AX staining [29]. Moreover, when a site-specific DSB is induced by expressing the HO endonuclease in yeast, γ -H2AX has been shown by chromatin immunoprecipitation (ChIP) to associate with DNA adjacent to the break [31,32,33]. Over time, the γ -H2AX can be immunoprecipitated with genomic loci increasingly distal from the HO break, up to 50 kilobases away [32].

γ -H2AX appears to be important for promoting efficient repair in both mice and yeast. Although, H2AX^{-/-} knockout mice are viable, although they are sensitive to IR [30]. H2AX^{-/-} mouse embryonic fibroblasts (MEFs) have more spontaneous chromosomal aberrations than their wild-type counterparts and generate more breaks when exposed to

IR. H2AX^{-/-} cells are also slower than H2AX^{+/+} cells in repairing IR-induced damage [30]. Similar phenotypes were observed in yeast carrying an H2A serine to alanine (AQ) mutation, which prevents H2A from being phosphorylated in response to damage. Studies examining *S. cerevisiae* and *S. pombe* H2A-AQ mutants report increased sensitivity to several DNA damaging agents, such as MMS, camptothecin, and IR, all of which generate DSBs [34]. This sensitivity is far less than that conferred by checkpoint and repair mutants, suggesting γ -H2AX contributes to, but is not essential for, both processes.

One mechanism by which γ -H2AX could promote repair is to recruit repair machinery to damage sites. DSBs are repaired by non-homologous end joining (NHEJ) and homologous recombination (HR). NHEJ promotes the re-ligation of two broken ends of a DSB, whereas HR uses a homologous template, preferably a sister chromatid, for repair-induced replication leading to rejoining of the broken ends. Localization studies of repair proteins argue against the notion that γ -H2AX is required for recruiting HR proteins. The HR protein Rad51 forms IR-induced foci in H2AX^{-/-} mouse MEFs [30] (Celeste et al., 2002). Similarly, the *S. pombe* HR protein Rad22 forms foci equally well in wild type or H2A-AQ mutants after exposure to IR [35]. The yeast MRN complex functions in both NHEJ and HR; whereas the role of this complex in mammalian DNA repair is less well understood. Published reports have shown an initial recruitment followed by a partial or complete loss of focus formation for the MRN proteins in H2AX^{-/-} cells [29,30,36]. As with recruitment of the checkpoint adaptors (below), this may indicate that the MRN complex has both an initial means of localizing to breaks (independent of γ -H2AX), and a secondary binding interface (dependent on γ -H2AX).

This latter interaction could be through a direct association of Nbs1 with γ -H2AX [36]. Since the MRN complex also targets ATM to damage sites, this might allow γ -H2AX to spread via a sequential cycle of phosphorylation and binding.

One compelling link to repair is not through recruitment of HR or NHEJ repair components themselves, but rather through the γ -H2AX-dependent association of cohesins to DSBs [32,37]. Cohesin complexes are the physical link between sister chromatids that maintain cohesion until mitosis occurs. It had been previously reported that cohesion is established during S phase. Recent studies in *S. cerevisiae* demonstrate that cohesin complexes can, in fact, be loaded *de novo* outside of S phase in response to an HO-induced DSB [32,37]. ChIP experiments demonstrate that this new loading occurs proximal to the HO break site, spanning an area that overlaps with γ -H2AX spreading. This cohesin loading is entirely dependent upon H2A phosphorylation [32]. Furthermore, repair of IR damage is slower in the absence of *de novo* cohesin loading, suggesting that cohesion promotes HR when a sister chromatid is used as a template [37].

An emerging picture of γ -H2AX function is that it promotes effective repair in multiple ways. Although it is clear that γ -H2AX is not essential for checkpoint signaling, several lines of evidence suggest that γ -H2AX may also promote the accumulation of checkpoint adaptors. The characterization of mouse H2AX^{-/-} cells demonstrated that, although these cells had a slight repair defect, they were still capable of eliciting a checkpoint response to high dose IR [30]. Nevertheless, they were defective in triggering the G2/M checkpoint when treated with low dose IR. Despite having a partially functional checkpoint, damage-induced foci of the checkpoint effectors NBS1, 53BP1, and BRCA1, all of which carry BRCT domains, were greatly diminished [29]. More

detailed analysis showed that these proteins could transiently form foci after damage induction without H2AX, but this localization was not sustained, suggesting a role in maintenance of the checkpoint [29]. Curiously, the role of the BRCT domain itself in γ -H2AX binding differs between proteins. NBS1, 53BP1, and a recombinant protein containing the BRCT (and FHA) domains of Nbs1 have each been shown to bind a phospho-H2A peptide. However, while the BRCT domain is important for NBS1 binding to a phospho-H2A peptide, 53BP1's BRCT domain is not required for its γ -H2AX binding or focus formation [38].

γ -H2AX also appears to have a role in adaptor function in *S. pombe*. After low levels of IR, the H2A-AQ mutant can appropriately phosphorylate downstream checkpoint components and is able to mediate a checkpoint arrest [35]. This checkpoint competency is challenged with increasing amounts of irradiation. However, H2A-AQ mutants cannot form Crb2 foci at sites of damage. Crb2 is able to bind to phosphorylated, but not unphosphorylated, H2A peptides *in vitro*, suggesting a direct interaction [35]. Thus, γ -H2AX is important, but not essential, for Crb2 response at DSBs.

Chromatin remodeling complexes are an additional class of proteins that appear to participate in DNA damage repair. An H2A S129E mutant in *S. cerevisiae*, which mimics a phosphorylated H2A histone, yields plasmids with less compacted chromatin than wild type, suggesting a link between γ -H2AX and chromatin structure [34]. More recently, three separate *S. cerevisiae* remodeling complexes, namely the NuA4, Ino80, and Swr1, have been shown to specifically interact with γ -H2AX or a phospho-H2A peptide [31,33,39]. NuA4 is a histone acetyltransferase complex whose catalytic subunit, Esa1, acetylates the N-terminal tail of H4, which is important for resistance to DNA-damaging

agents [40]. The Ino80 and Swr1 complexes both contain a catalytic subunit in the SWI/SNF family of ATP-dependent chromatin remodeling enzymes. The Ino80 complex can remodel and slide nucleosomes *in vitro*, whereas the Swr1 complex exchanges H2A for H2AZ *in vitro* and *in vivo* [27,41]. These complexes are localized to DNA proximal to an induced HO break. Preventing the function of Ino80, NuA4, or Swr1 sensitizes cells to DSB-inducing agents [31,33,39,40].

Ino80, NuA4, and Swr1 could promote access to or processing of DNA by repair proteins. Chromatin remodeling may also lead to the removal of phosphorylated histones. This intriguing activity has been recently suggested by Kusch et al., who examined the *Drosophila melanogaster* Tip60 chromatin remodeling complex, which contains subunits homologous to both the yeast NuA4 and Swr1 complexes [42]. Tip60 specifically acetylates the phosphorylated form of the fly histone variant H2Av (a.k.a. H2AvD) and this acetylation promotes the removal of phospho-H2Av from nucleosomes. H2Av is phosphorylated upon damage in a manner analogous to H2AX but also has characteristics of H2AZ. Loss of Tip60 *in vivo* results in the persistence of damage-induced phospho-H2Av foci [42], presumably because of a lack of H2Av eviction. However, it is not yet known whether this exchange promotes repair or simply allows cells to recover after repair. Furthermore, it is unclear whether damage induced exchange is a property of mammalian H2AZ or H2AX, since H2AX is reported to be immobile in chromatin [28].

Histone methylation

Histone methylations are best known for their role in gene silencing and

heterochromatin formation. These post-translational modifications are carried out by Histone Methyl-Transferases (HMT), which covalently modify lysines and arginines on histones. Specifically, histones H3 and H4 are methylated on multiple residues and often times a single lysine can have mono-, di-, or tri-methylations. These modifications, in combination with acetylations, are thought to inscribe a histone pattern that recruits factors that affect transcription. For example, in both yeast and mammals, methylation of lysine 9 on H3 recruits heterochromatin protein 1, which is necessary for silencing. In other cases, methylated histones can recruit more HMTs to act on the same or neighboring histones [41]. Recently, histone methylations have been implicated in the DNA damage checkpoint and repair pathways.

Bulk levels of histone methylations do not appear to be induced after DNA damage [43]. Nonetheless, histone methylations contribute to the checkpoint by directly interacting with checkpoint components. The checkpoint proteins Rad9/Crb2/53BP1 have been suggested to be recruited to damage sites by histone methylations. In mammals, methylation of lysine 79 on H3 (H3-K79-Me) is important for localization of 53BP1 [43]. Cells deficient in Dot1, the HMT responsible for lysine 79 methylation, are unable to form 53BP1 foci after damage. The requirement for H3-K79 methylation in 53BP1 focus formation is most likely due to a direct interaction between H3 and 53BP1, since 53BP1 can bind H3-K79-Me *in vitro* [43].

S. cerevisiae seems to share this mechanism. Mutants deleted for *DOT1* or unable to be methylated at lysine 79 (H3-K79A) show a decrease in the kinetics of radiation-induced Rad53 phosphorylation (a readout for checkpoint activation) after DNA damage [44]. Ubiquitination of H2B by Rad6-Bre1 is required for H3-K79 methylation and

blocking this step similarly reduced Rad53 phosphorylation and its *in vitro* kinase activity after DNA damage [44]. As with 53BP1, Rad9 binds H3 *in vitro* [43]. Similar to the loss of γ -H2AX, deletion of *DOT1* or *RAD6* does not entirely eliminate the checkpoint, suggesting that an independent mechanism for the recruitment of Rad9 must exist [44].

S. pombe also uses histone methylation to recruit the adaptor protein Crb2 to damage, although it apparently uses a different methylation site, lysine 20 on histone H4 [45]. The methylation on H4-K20 requires the HMT Set9, and studies have shown that *set9*-deleted cells were more sensitive than wild type to several types of damage. *crb2* mutants are much more damage sensitive than *set9* (or H2A-AQ) mutants, consistent with the model of alternative recruitment mechanisms for adaptor proteins. The number of Crb2 foci is reduced in cells lacking *SET9* [45], and the G2 checkpoint is partially defective, as indicated by premature entry into mitosis. Moreover, the downstream checkpoint kinase Chk1 accumulates in its unphosphorylated form, also suggesting defects in checkpoint signalling. However, a complete loss of checkpoint function was only seen when a *set9* deletion was combined with mutations in other checkpoint genes.

From the examples above, it is evident that histone methylations play a part in the DNA damage checkpoint pathway, even though the methylation sites used are not entirely conserved. Mammals and budding yeast employ H3-K79-Me, whereas *S. pombe* uses H4-K20-Me. Despite this, the tandem Tudor domain, which is found in each of these checkpoint adaptor proteins and is thought to bind the methylated histone, is conserved [43]. Tudor domains have been characterized in several proteins that recognize methylated proteins, and have structural and sequence similarities to other methyl-binding domains, such as Chromo domains. Huyen et al. showed that mutants in the

Tudor domain of 53BP1 eliminate its ability to form damaged-induced foci and bind H3-K79-Me containing chromatin *in vitro* [43].

Conclusions

Collectively, these data represent a complicated picture of Rad9/Crb2/53BP1 recruitment (Fig 1a). The complication stems largely from three facts. First, the recruitment of the adaptor proteins appears to depend upon many different modifications, only a subset of which are known to be DNA damage inducible. Second, some of these modifications seem to recruit several proteins to chromatin, leaving open the possibility that the observed dependencies could be indirect. Finally, neither chromatin remodeling nor histone modifications are absolutely required for these adaptor proteins to function in the DNA damage response.

In an effort to combine these data into a coherent picture, we present a speculative model (Fig. 1b). Upon induction of a DSB, ATM initially associates with DSB ends and phosphorylates H2AX. After the initiation of resection, ATM is replaced in part by ATR, which maintains and expands the γ -H2AX phosphorylation. γ -H2AX then recruits several chromatin remodelers, including the Ino80 and Nu4A complexes. The activity of these complexes may promote the exposure of pre-existing H4-K20-Me or H3-K79-Me modifications on nearby nucleosomes or could facilitate repair. Recruitment of Rad9/Crb2/53BP1 could then be driven by a cooperative association of these adaptors with both γ -H2AX and K-Me histone in a manner that may be aided by remodeling enzymes. Regardless of the exact mechanism, the data reviewed here places the majority of the recruited Rad9/Crb2/53BP1 at the unresected, intact chromatin, significantly distal

to the ssDNA-associated Mec1/Rad3/ATR kinase.

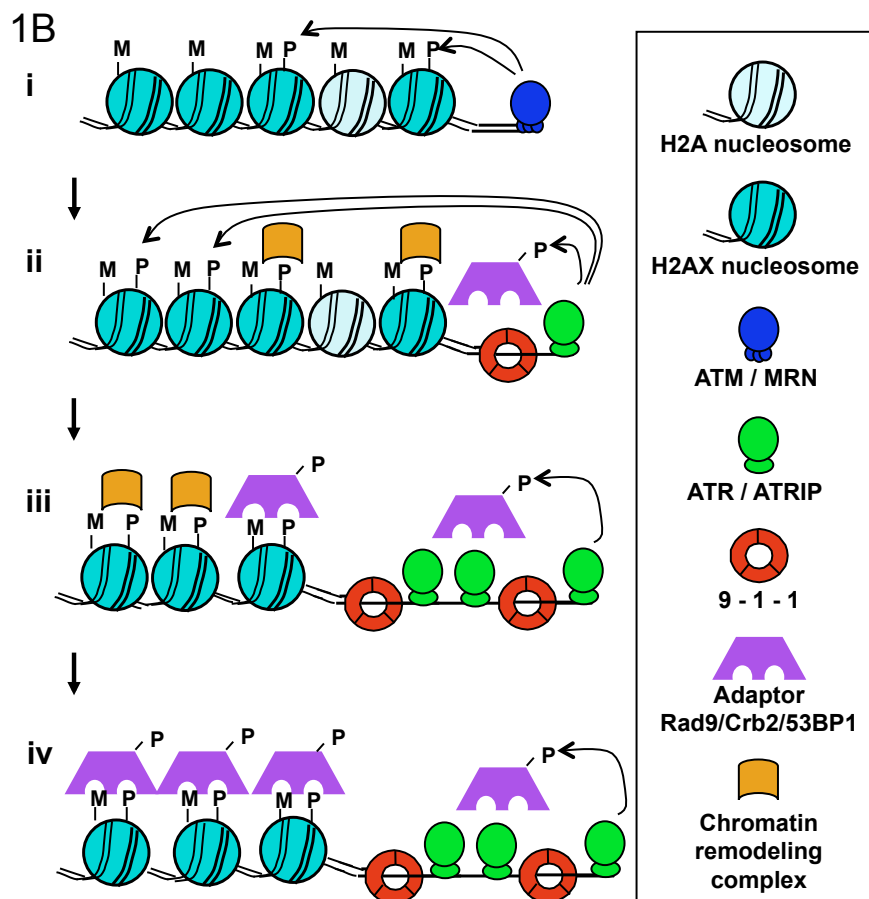
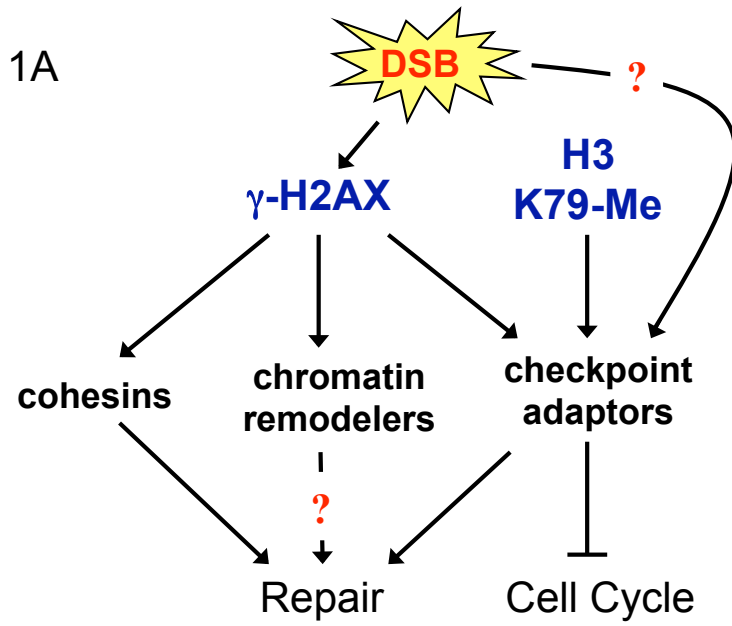
The use of a constitutive histone modification to mediate the binding of checkpoint proteins to DNA damage sites is both intriguing and confusing. In yeast, K79 methylated H3 is abundant and accounts for ~90% of the H3 in the cell [46]. Thus, K79 methylated H3 may simply be part of a constitutive protein/protein interaction domain. Alternatively, methylation of H3-K79 could furnish an added level of regulation. H3-K79 is undermethylated at telomeres and some silenced regions [47]. Moreover, it is not yet known whether the level of H3-K79 methylation proximal to a DSB is altered. However, the fact that most of the genome is bound to K79 methylated H3 strongly suggests that this modification is not sufficient to target the adaptors to DSBs in the absence of γ -H2AX.

Despite the fact that loss of either H2AX phosphorylation or H3-K79-Me/H4-K20-Me compromises Rad9/Crb2/53BP1 function, these checkpoint adaptors still respond to DNA damage and, at least in the case of Rad9 and Crb2, have been shown to retain an active function in the checkpoint pathway. Further experiments may show that Rad9/Crb2/53BP1 activity is entirely eliminated by the simultaneous disruption of both γ -H2AX and H4-K20/H3-K79 methylation. Alternatively, Rad9/Crb2/53BP1 might remain damage-responsive in these mutants because it has another mechanism for associating with damage sites, independent of nucleosomes. For example, Rad9/Crb2/53BP1 could associate with the resected ssDNA, either directly or through an association with other checkpoint proteins. Were this the case, the ssDNA-associated fraction would likely represent a minority of the DSB-associated Rad9/Crb2/53BP1, since γ -H2AX can spread 25 kilobases before resection has extended more than a few

kilobases. Thus, the majority of the signal detected for these adaptors in focus formation assays would be lost in cells lacking these histone modifications, even though a significant functional pool might be retained. Why, then, is it critical to create a local pool of checkpoint adaptors through multiple means of recruitment? Is the chromatin-associated adaptor functionally distinct and acting at a different step in the checkpoint pathway? The answers to these questions will have to await further studies to unravel these complicated tails.

Figure legend

Models of recruitment to a DSB via histone modifications. 1A. γ -H2AX is induced by DSBs to recruit cohesins, chromatin remodeling complexes, and checkpoint adaptors to the damage site. The H3-K79-Me (H4-K20-Me in *S. pombe*) is a constitutive modification that contributes to recruiting checkpoint adaptors to DSBs. **1B.** (i) The ATM kinase is recruited to the broken end through the MRN complex, where it mediates H2AX phosphorylation. (ii) After the initiation of resection, both ATR (and its associated ATRIP subunit) and 9-1-1 are recruited to the resected area adjacent to the break. ATR phosphorylates the adaptor protein and expands upon the initial H2AX phosphorylation. Chromatin remodeling complexes, such as NuA4, are recruited to γ -H2AX. (iii) Chromatin remodelers facilitate presentation of H3/H4 methylations. (iv) Adaptors interact cooperatively with H3/H4 methylation and γ -H2AX.



Chapter 3

Calling 9-1-1:

Recruitment of the 9-1-1 Complex to DNA Damage

INTRODUCTION

The presence of DNA damage, such as a double-strand break (DSB), elicits a vital checkpoint response that recognizes the damage and activates a signaling pathway to arrest cell cycle progression. In the budding yeast *S. cerevisiae*, two checkpoint protein complexes, Mec1-Ddc2 and Ddc1-Rad17-Mec3 (Rad9, Hus1, and Rad1 in higher eukaryotes, referred to as the 9-1-1 complex) are recruited independently to DNA damage and initiate the checkpoint-signaling pathway [2,3]. The recruitment of these two complexes to damage sites has been observed to form damage induced foci, or “damage foci,” *in vivo* by fluorescence microscopy with the use of Ddc1-GFP and Ddc2-GFP fusion proteins. In *S. cerevisiae*, a useful system has been developed to generate a DSB by galactose-inducible expression of the HO endonuclease. The endogenous HO-recognition sequence was deleted and an ectopic site was introduced at the telomere of chromosome VII. This system provides a unique opportunity to monitor the events that occur at a single site-specific break that cannot be repaired by homologous recombination. Both Ddc1-GFP and Ddc2-GFP exhibit diffuse nuclear localization in the absence of damage. However, when an HO-induced DSB is generated, one nuclear Ddc1-GFP or Ddc2-GFP focus forms, suggesting that many molecules of either complex can aggregate to the single break [1]. This raises the question, how can one DSB support the accumulation of multiple checkpoint complexes?

Various groups have suggested that checkpoint proteins recognize the signal produced by the processing of damaged DNA rather than the damage *per se*. When a DSB occurs, the lesion undergoes 5′ to 3′ resection to produce long stretches of single-stranded DNA (ssDNA) with a 3′ overhang. Checkpoint signaling by the epistasis group

that includes DDC1, RAD17, MEC3, and RAD24 correlated with the generation of ssDNA from telomere (DSB-like) damage [48]. Zou and Elledge [5] demonstrated in *S. cerevisiae* that RPA, an ssDNA binding protein, bridges the association between the Mec1-Ddc2 and ssDNA *in vitro* and *in vivo* (Figure 1). They demonstrated that this requirement for RPA is true for the mammalian homolog ATR/ATRIP as well. The substrate that targets the other checkpoint sensor, Ddc1-Rad17-Mec3, to ssDNA remains to be determined.

A subset of checkpoint proteins bears remarkable parallels with replication proteins. During replication, the Pol α -primase complex provides the initial RNA primer and short DNA extension required to initiate DNA synthesis. The heteropentameric RFC complex, or clamp loader, then recognizes the 3' ssDNA/dsDNA primer-template DNA and loads PCNA onto dsDNA at these replication-intermediate sites. PCNA is the homotrimeric ring-shaped protein that is clamped around and slides about DNA, and tethers the replicative DNA polymerase to its substrate [49]. The checkpoint proteins Ddc1, Rad17, and Mec3 form a PCNA-like clamp that is similarly loaded around DNA. An alternative clamp loader also exists in which the checkpoint protein Rad24 substitutes for the replication-Rfc1 subunit in complex with Rfc2-5 [50,51]. *In vitro* experiments provide evidence that the Rad24-RFC complex indeed acts as a specific clamp loader to its respective checkpoint clamp and requires a primed template [4,51,52,53]. However, these data provide contradictory evidence as to whether the checkpoint clamp has a higher specificity for 5' ssDNA/dsDNA junction created by resection or 3' replication-like junctions. Therefore, the specific *in vivo* substrate onto which the checkpoint clamp is loaded remains to be determined.

To investigate the mechanism for *in vivo* checkpoint clamp loading, we utilized the inducible-HO endonuclease system to monitor localization of proteins to a DSB site. We found that RPA but not components of Pol α -primase localized to a break and are required for the recruitment of checkpoint clamp. GFP fusions to RPA subunits, Rpa1 and Rpa3, formed a bright focus with the induction of an HO break. A temperature-sensitive allele of RPA, *rfa1-Y29H*, diminished the ability of Ddc1-GFP to form damage foci, suggesting that, similarly to the other checkpoint sensor Ddc2, Ddc1 recognized the ssDNA binding protein. However, unlike its replication-counterpart PCNA, Pol α -primase was not required for either Ddc1-GFP damage-foci formation or checkpoint arrest. By chromatin immunoprecipitation (ChIP), the recruitment pattern of both Ddc1 and Ddc2 to the HO break on chromosome VII matched that of RPA, implying both checkpoint sensors are recruited along the ssDNA exposed by resection.

RESULTS

RPA forms damage-induced foci and is required for checkpoint sensor localization.

In vitro loading of the replication clamp utilizes both RPA and Pol α -primase [49]. RPA consists of three subunits, Rpa1-3, that collectively bind ssDNA. Pol α -primase has both polymerase and primase functions and consists of 4 subunits: Pol1 is the catalytic-polymerase subunit; Pol12 is a regulatory subunit of the polymerase; Pri1 is the catalytic primase subunit; and Pri2 is the non-catalytic primase subunit. To determine if these complexes might also be involved with *in vivo* checkpoint clamp loading, we first examined if GFP fusions to subunits of RPA and Pol α -primase respectively, localize to

DSBs like Ddc1-GFP. As previously published, Ddc1-GFP forms a single GFP focus in cells expressing the HO endonuclease to create a single DSB (Figure 1A) [3]. Similarly, two subunits of RPA, Rpa3-GFP (Figure 1) and Rpa1-GFP (data not shown) readily form a single-GFP focus when an HO break is induced. However, none of the Pol α -primase subunits examined: Pri2- (Figure 1A), Pol1-, nor Pol12 –GFP (data not shown) form HO-induced foci.

To determine if RPA localization to DSBs has functional significance to *in vivo* Ddc1 loading, we examined how a temperature-sensitive allele of the large RPA subunit, *rfa1-Y29H*, affects checkpoint sensor localization. As expected, zeocin-induced Ddc2-GFP foci did not form when *rfa1-Y29H* cells were shifted to the non-permissive temperature of 36°C (Figure 1B). Similarly, *rfa1-Y29H* prevented Ddc1-GFP from forming foci in zeocin-treated cells. Not only does RPA itself localize to either HO- or zeocin-induced DSBs, it is also required for both Ddc1 and Ddc2 to be recruited to breaks.

Pol α -primase does not participate in the DNA-damage checkpoint

The inability to visualize Pol α -primase damage-induced GFP foci may be because the number of accumulated molecules fell below threshold of visual detection. To get around this complication, we instead determined if Pol α -primase has a functional role in checkpoint localization. We examined the effect of expressing a catalytically-dead allele of the polymerase subunit, *poll-cd*, or wildtype on Ddc1 localization to an HO break. If the Pol α -primase was producing primers along the ssDNA created from resection at a DSB, we expected that expressing the catalytically-dead allele of *POL1*

would act dominantly to the endogenous protein. However, we found that Ddc1-GFP was still able to form HO-induced foci (Figure 1A). Unlike RPA, Pol α -primase is not required for *in vivo* recruitment of the checkpoint clamp to a DSB.

Pol α -primase exhibits cell-cycle dependent localization patterns.

Although Pri2 Pol α -primase subunit did not exhibit damage-dependent foci like the checkpoint sensors, we observed that it did, however, display cell-cycle dependent localization patterns. To further investigate this observation, we additionally examined other Pol α -primase subunits, Pol1-GFP and Pol12-GFP. In G2/M arrested cells due to zeocin and nocodazole treatment, Pol1-GFP remained nuclear but seemed to be enriched along the nuclear periphery (Figure 2B). The Pol12-GFP subunit displayed similar localization patterns. In asynchronous cells, Pol12-GFP had a mixed localization pattern: diffusely nuclear with brighter concentrated GFP patch in G1/S cells (marked by a single nucleus) or lightly nuclear with enrichment at the nuclear periphery in a G2/M cells (dividing nucleus) (Figure 2C). These localization phenotypes were more dramatic in cells synchronized in G1 and G2 with α -factor and nocodazole, respectively (Figure 2C). To compare, we also visualized the localization of Nup170-GFP, a nuclear-pore component, which served as a control for the nuclear periphery (Figure 2D). It appears that Pol α -primase is diffusely nuclear in G1/S but then relocates to the nuclear periphery as cells progress into the G2/M stage of the cell cycle, which is consistent with later observations [54].

Checkpoint arrest requires RPA but not Pol α -primase

We examined various temperature-sensitive alleles of RPA and Pol α -primase to determine if their effect on checkpoint sensor localization also correlates with their ability to elicit a checkpoint response. To circumvent the essential role of these two complexes in replication, cells were pre-synchronized in G2/M with nocodazole before shifting to the non-permissive temperature of 36°C for 30 minutes. Damage was induced with or without zeocin for another 30 minutes before cells were washed, resuspended in trapping medium, which was prewarmed to 37°C and contained α -factor +/- zeocin, and fixed at various times after nocodazole release. Checkpoint arrest was measured by counting the percentage of DAPI-stained cells that remained large-budded with a single nucleus. Wildtype cells that were treated with or without zeocin served as the controls for checkpoint arrest or cell division under these conditions, respectively. We expected that other Pol α -primase ts mutants would not display checkpoint defects, given overexpression of the catalytically-dead allele of *POL1* had no effect on Ddc1-GFP localization (Figure 2A). Consistent with this hypothesis, both the *pri1-M4* (Figure 3A) and the *pri2-1* (Figure 3B) strains were able to elicit a checkpoint arrest to the same extent as damaged-wildtype strains. The *pri1-M4 rad24 Δ* and the *pri2-1 rad24 Δ* double mutants continue with the cell cycle much like undamaged wild-type cells (Figures 3A and 3B) or like the checkpoint-defective *rad24 Δ* single mutant (not shown). In contrast, the *rfa1-Y29H* mutant displayed a checkpoint defect that was equivalent to the *rfa1-Y29H rad17 Δ* double mutant and undamaged wildtype cells (Figure 3B). In agreement to their effect on Ddc1-GFP localization, RPA but not Pol α -primase is essential to mediate a DNA damage checkpoint arrest.

RPA, Ddc1, and Ddc2 localize to a DSB and spread distally over time.

In addition to GFP localization, both Ddc1 and Ddc2 have previously been shown to localize to HO breaks by chromatin immunoprecipitation (ChIP) [2,3,5]. However, we wanted to further explore the nature of the recruitment of these checkpoint proteins.

Using the engineered-telomeric HO site on chrVII, we monitored RPA, Ddc1, and Ddc2 binding by ChIP along chrVII over time. The inducible HO endonuclease was expressed continuously throughout the course of the experiment to prevent the possibility of repair. Primer pairs for quantitative PCR (QPCR) were designed to amplify 300 bp regions at 1kb intervals that span as far as 50kb from the break site on chrVII. The control primer pair for all ChIP experiments amplified a region within the *NUP170* locus on chrII.

ChIP of Rpa3-GFP gave early and increasingly robust signal, likely due to the direct interaction with ssDNA (Figure 4A). An hour after HO induction, RPA associated with DNA up to 4kb away from the HO-break site. The rate at which RPA binding was observed to spread along chrVII was consistent with the previously estimated resection rate of 2-4 kb/hr (Haber?). Not surprising, Ddc2-TAP recruitment to the HO break similarly spread distally from the break, albeit slower than RPA (Figure 4B). By the 6 hr time point, RPA was detected as far as 50kb from the break whereas Ddc2 was only beginning to be detected around 14kb (Figures 4A and 4B). The nearly ten-fold drop in Ddc2 ChIP signal compared to RPA may be due to the indirect contact of Ddc2 to DNA via RPA. The ChIP profile of the checkpoint clamp subunit, Ddc1-TAP, appeared to closely mimic distal RPA spreading (Figure 4C). Like RPA, Ddc1 bound chrVII 25-50kb away from the break (Figure 4A and 4C). A similar distal spreading of Ddc1-TAP ChIP was observed from strains that utilize the endogenous HO-recognition site on chrIII

(Figure 5A). Both checkpoint sensors associate with DNA proximal to a DSB and spread distally.

***In vivo* recruitment of Ddc1 at sites of ssDNA**

The parallel ChIP profiles of Ddc1 and RPA suggest that Ddc1 is recruited along ssDNA like RPA. To check specifically, we measured the amount of ssDNA produced along an HO-induced DSB. Initial experiments were conducted in strains carrying the HO break on chrVII. However, in developing an assay to measure ssDNA, we discovered that the HO cutting was inefficient at this site. Oligos were designed to flank the HO restriction site that would only give QPCR product with intact DNA and no product upon cutting. We found that after an hour of HO induction, there was approximately 70% retention of the HO site on chrVII, whereas strains with the endogenous chrIII site displayed less than 5% retention (data not shown). These results prompted us to repeat the Ddc1-TAP ChIP experiments in strains with the chrIII HO site. The chrIII HO break site has the added benefits of bearing the full endonuclease recognition sequence and allows for ChIP analysis on either side of the break. In these strains, Ddc1-TAP showed similar distal spreading on both sides of the chrIII HO break (Figure 5A). In addition, the signal from the ChIP was at least three-fold higher than those gathered from the strain with the chrVII break, adding to the evidence that HO cutting in the engineered strains was less efficient.

To monitor the amount of ssDNA generated from resection, we created a PCR ssDNA protection assay. DNA isolated from the ChIP experiments were subjected to TaqI endonuclease digestion, which should only cut double-stranded DNA. TaqI was

chosen because it is active at 65°C, which would prevent the possibility that it could digest secondary structures that might arise from the ssDNA, and it has a four-base recognition sequence that will ensure that it will cut often. The digested DNA served as template for QPCR and should only produce products if ssDNA protected against TaqI digestion or if TaqI did not cut within the region amplified by the primers. Chromosomal sequence was analyzed before performing the assay to ensure the presence of TaqI restriction sites within the targeted PCR-amplification regions. Utilizing the ssDNA protection assay on the strain with the chrIII HO site, we found that after 6 hours of HO expression, ssDNA could be detected as far out as 20 kb from the break (Figure 5B). The highest percentage of ssDNA measured at from the break reached up to 40%, levels that were consistent with other PCR-based assays used to measure ssDNA generated from telomeric DSB-like damage (Lydall-QAOS). PCR across the break site indicated if the break indeed occurred (Figures 5A and 5B). The low percentage of ssDNA found immediately proximal to the break may be indicative of decreased ssDNA stability after extended timepoints. Collectively, these data suggest that Ddc1 localizes to a break and spreads along ssDNA regions.

DISCUSSION

The loading of the replication PCNA clamp has been extensively studied *in vitro*, demonstrating the RFC clamp loader binds at ssDNA/dsDNA junctions, opens the PCNA ring, and loads PCNA to encircle dsDNA. RFC specifically recognizes 3' primer-template ssDNA/dsDNA junctions created by Pol α -primase *in vivo*. PCNA is able to slide along dsDNA but not ssDNA [49], contributing to its function as a polymerase

processivity factor. The checkpoint clamp, 9-1-1, loading has been similarly studied to determine what provides the *in vivo* specificity for two very different processes: replication and checkpoint activation. Like PCNA, the 9-1-1 clamp is opened to encircle DNA by its checkpoint specific Rad24/RFC2-5 clamp loader and can also slide along dsDNA. The difference in specificity most likely depends on the orientation of the ssDNA/dsDNA junction. The process of resection, which occurs in a 5' to 3' direction, creates a 5' ssDNA/dsDNA junction for the checkpoint clamp and clamp loader. There are some conflicting data, but *in vitro* studies report that the Ddc1-complex can indeed be loaded onto these 5' junctions but may also retains some affinity for 3' junctions [4,51,52,53]. While this model provides a specificity difference for substrates, it introduces a question of how can enough Ddc1 molecules accumulate to a break when only one junction on either side of the break is available for 9-1-1 loading?

We tested the hypothesis that the replication proteins RPA and Pol α -primase were required for checkpoint activation. The model we considered was that RPA and Pol α -primase produced replication-like intermediates, primers along the ssDNA revealed from resection, as a means to amplify 9-1-1 loading by providing multiple loading junctions rather than the two created by resection on either side of a DSB. Pol α -primase neither localized to sites of DNA damage nor was genetically required to elicit a checkpoint response. We did however uncover a previously uncharacterized localization pattern of Pol α -primase based on cell-cycle position that will be discussed below. Unlike Pol α -primase, the replication protein, RPA, is required for both checkpoint arrest and Ddc1-focus formation. Cells deleted of either *DDC1* or *DDC2* are incapable of triggering a checkpoint arrest [55,56]. Thus, the checkpoint defect of *rpa1-Y29H* may be attributed to

loss of either Ddc2/Mec1 or 9-1-1-clamp localization to a break alone. However, the recruitment of Ddc2/Mec1 and 9-1-1 to damage occurs independently of each other [2,3], suggesting RPA is indeed required for Ddc1 localization. The profile of recruitment and spreading to an HO break, by ChIP, was strikingly similar between RPA and Ddc1 (Figures 4A and 4C). The accumulation of Ddc1 proximal to an HO break also corresponds with the generation of ssDNA (Figure 5).

The simple model that stems from these observations would suggest that ssDNA, mediated by RPA, is the signal that recruits checkpoint sensors to damage sites to initiate checkpoint signaling. However, several mechanistic details remain unresolved. *In vitro* sliding experiments suggest 9-1-1 is loaded onto dsDNA from the ssDNA/dsDNA junctions [51], but our data suggest 9-1-1 associated with areas of ssDNA. Moreover, we ruled out the possibility that Pol α -primase could provide substrates onto which the clamp could be loaded. Is there a checkpoint alternative to Pol α -primase? If not, how then can 9-1-1 accumulate on ssDNA? Is 9-1-1 loaded at a resected junction, then left behind on ssDNA as resection continues? Alternatively, where does *de novo* 9-1-1 loading occurs long after resection has begun: only at the resection site or all along the already exposed ssDNA? We attempted to address the latter question by creating an inducible checkpoint-clamp loading system. However, we were unable to create a fully-repressible *RAD24* construct, the checkpoint-specific clamp-loader subunit, which was necessary for the experiment to be successful. Clearly, there are many questions that remain to understand the mechanism of checkpoint initiation.

As mentioned above, we discovered a previously uncharacterized localization pattern for Pol α -primase. Early in the cell cycle, from G1 to S phase, GFP fusions to

various Pol α -primase subunits appeared diffusely nuclear. Then as cells progress into G2/M, Pol α -primase became more concentrated at the nuclear periphery (Figure 2), observations that were later confirmed [54]. Pol12, a non-catalytic subunit of Pol α -primase, has previously been shown to be phosphorylated in a cell-cycle dependent manner [57] and the catalytic Pol1 subunit was determined to be an *in vitro* CDK substrate [16]. One of the many functions of CDK, as a critical cell-cycle regulator, is to prevent potentially lethal events such as re-replication from occurring [58]. We hypothesized that CDK-dependent phosphorylation of Pol α -primase was responsible for its localization pattern. We also proposed that the purpose of this perinuclear relocalization was to provide an additional control to prevent inappropriate re-replication. Pol α -primase was an excellent candidate to be an *in vivo* CDK target: the *POL1* subunit contained 2 full CDK consensus sites [S/T]-P-x-[K/R] and 11 additional proline-directed sites [S/T]-P; the *POL12* subunit contained 12 proline-directed sites. Further characterization of Pol α -primase was performed in collaboration with the J. J. Li lab. Mutation of all putative CDK sites on *POL12* (*pol12-12A*), but not *POL1* (*pol1-13A*), prevented Pol α -primase from localizing to the nuclear periphery in G2/M (personal communication, M. E. Liku and J. J. Li). Pol12 has been shown to form a constitutive complex with the other Pol α -primase subunits but its function has never been established. Our results provide a novel role for Pol12 in determining Pol α -primase nuclear localization. Regarding the purpose of relocalization, neither *pol12-12A* nor *pol1-13A* exhibited a re-replication phenotype. These two mutants were also unable to exacerbate the phenotype of known re-replication mutants (personal communication, M. E. Liku and J. J. Li). These preliminary results suggest Pol α -primase relocalization does not

contribute to re-replication inhibition. We speculate that, instead, Pol α -primase perinuclear association may facilitate replication of genomic loci, such as telomeres, that have been found to cluster near the nuclear periphery [59] and reported to have late-replication timing [60]. Pol α -primase associates with chromatin as early as G1 [61] and the G1 localization we observed consisted of a bright GFP patch and a weaker diffuse signal in the nucleus. Together, these data suggest that Pol α -primase is preferentially associated either with a subset of chromatin or perhaps more accessible chromatin, such as euchromatin. However, many more experiments are necessary to confirm these theories.

Figure Legends

Figure 1. RPA co-localizes to DSBs and is required for checkpoint localization. (A)

Cells were pre-grown in YM-1 raffinose medium before galactose was added to induce HO endonuclease expression. Localization of Ddc1-, Rpa3-, and Pri2-GFP proteins was analyzed by fluorescence microscopy after 3 hours of galactose treatment. The fluorescence exposure setting was constant between damage and undamaged samples, but was adjusted accordingly for each GFP-fusion protein. (B and C) Cells were synchronized in G2/M with nocodazole before adding zeocin at 23°C. After an hour of zeocin treatment, cells were shifted to the non-permissive temperature of *rfa1-Y29H*. The localization of (B) Ddc2-GFP and (C) Ddc1-GFP were analyzed after the third hour of zeocin treatment.

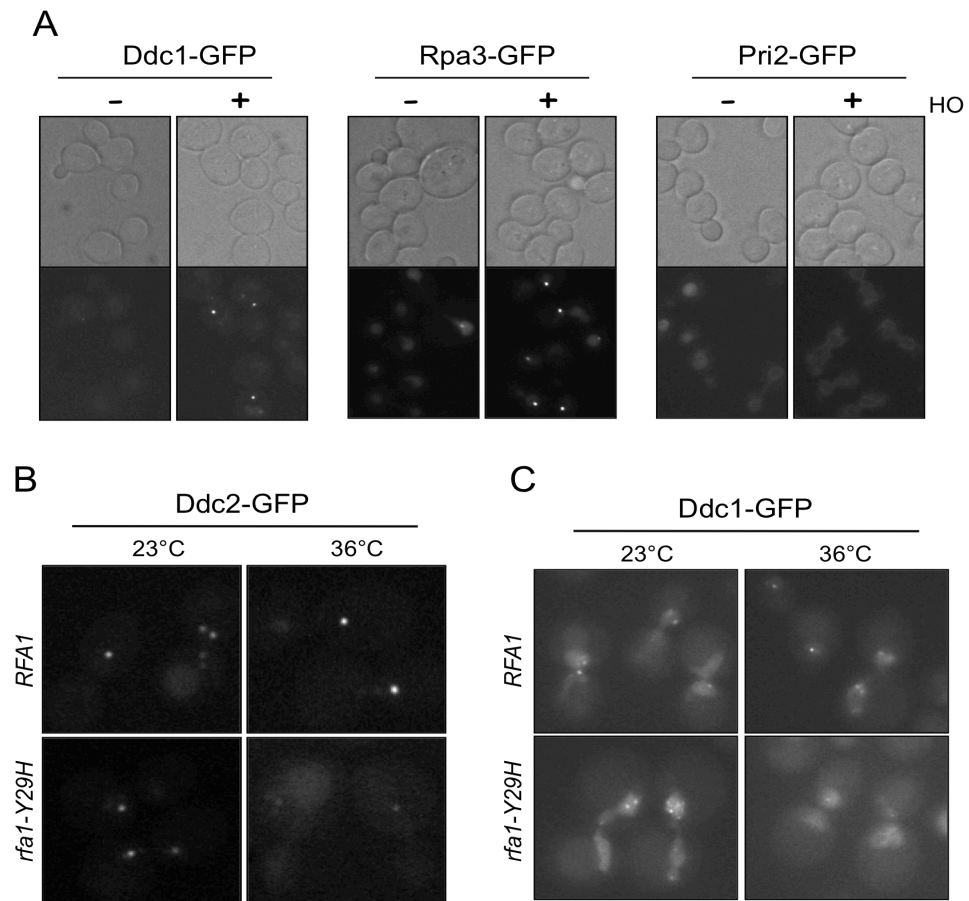


Figure 2. Pol α -primase displays cell-cycle dependent and DNA-damage independent localization patterns. (A) Ddc1-GFP was visualized in cells pre-arrested in nocodazole before adding galactose to induce both the HO break and *POL1* or *pol1-cd*, a catalytically-dead allele. (B) Localization of the Pol1-GFP in zeocin treated or nocodazole arrested cells. (C) Localization of Pol12-GFP, another Pol α -primase subunit, in asynchronous, G1 α -factor arrested, G2/M nocodazole arrested cells. (D) Nup170-GFP, a component of the nuclear pore complex, was visualized as a control for nuclear envelope localization.

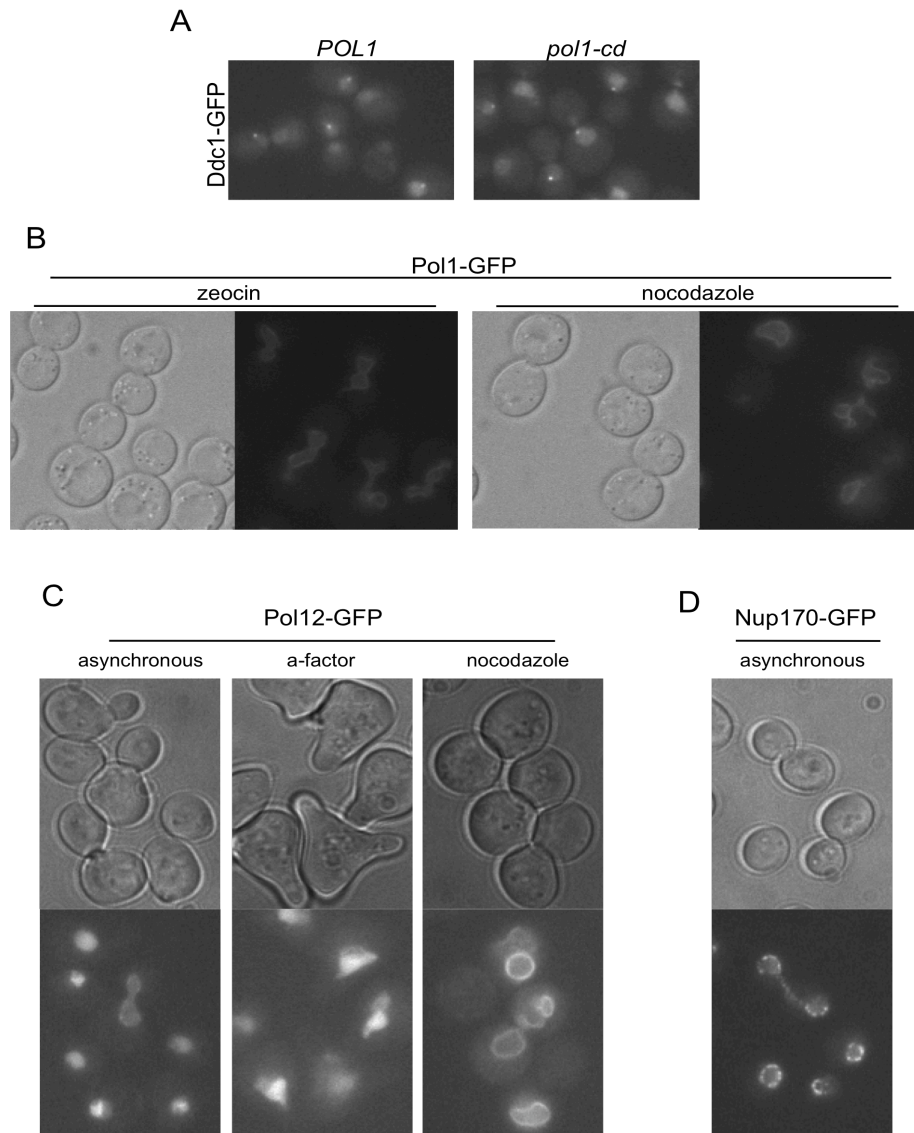


Figure 3. RPA but not Pol α -primase mutants display checkpoint defects.

Various temperature-sensitive replication mutants including (A) *pri1-M4*, (B) *pri2-1*, and *rfa1-Y29H* in combination with *rad24 Δ* or *rad17 Δ* were analyzed for checkpoint defects.

Cells were pre-arrested in nocodazole for 2.5 hours at 23°C, shifted to 37°C for 30

minutes, then treated +/- 0.2 mg/ml zeocin for an additional 30 minutes. Only wildtype

cells were treated (+/-) zeocin; all mutants were (+) zeocin. Cells were washed to remove

the nocodazole and resuspended in pre-warmed YM-1 containing 7.5 μ g α -factor +/-

zeocin trapping medium. Cells were collected at 10 minute intervals and fixed in 70%

EtOH. Checkpoint arrest was determined by DAPI staining for large-budded cells

containing an undivided nucleus.

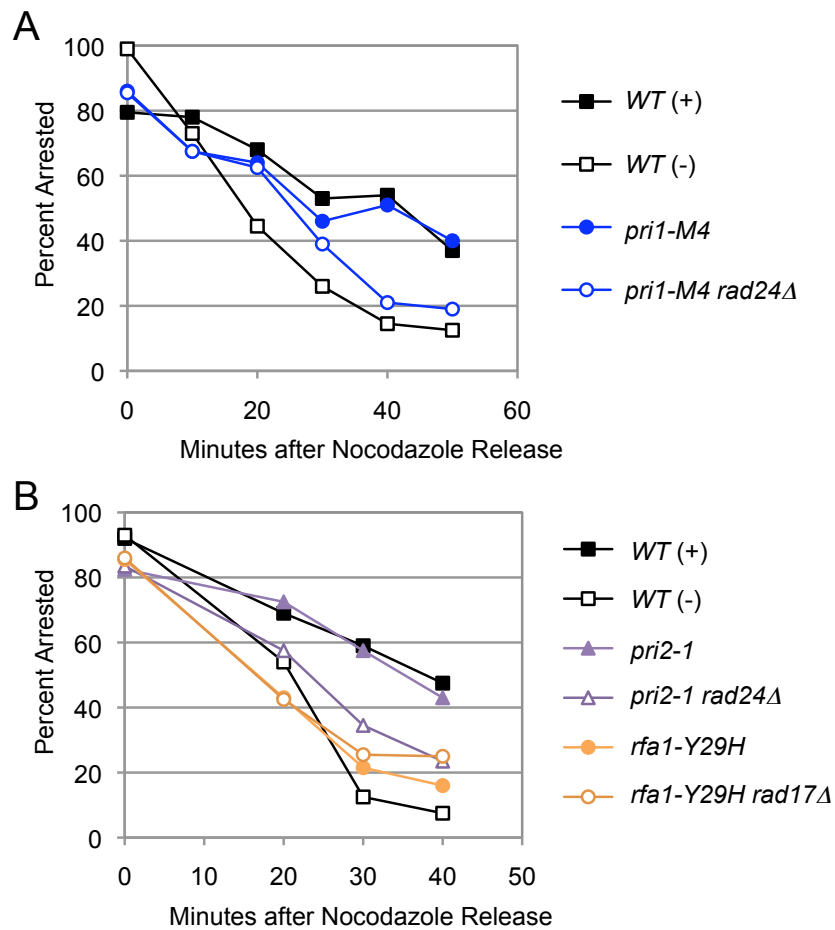


Figure 4. Distal spreading of RPA, Ddc1, and Ddc2 from an HO break. (A) Rpa3-GFP, (B) Ddc1-TAP, and (C) Ddc2-TAP were immunoprecipitated for ChIP analysis in strains harboring an engineered HO recognition site on chrVII. The QPCR primer pairs amplified in regions increasingly distal to the HO break and proximal to the centromere.

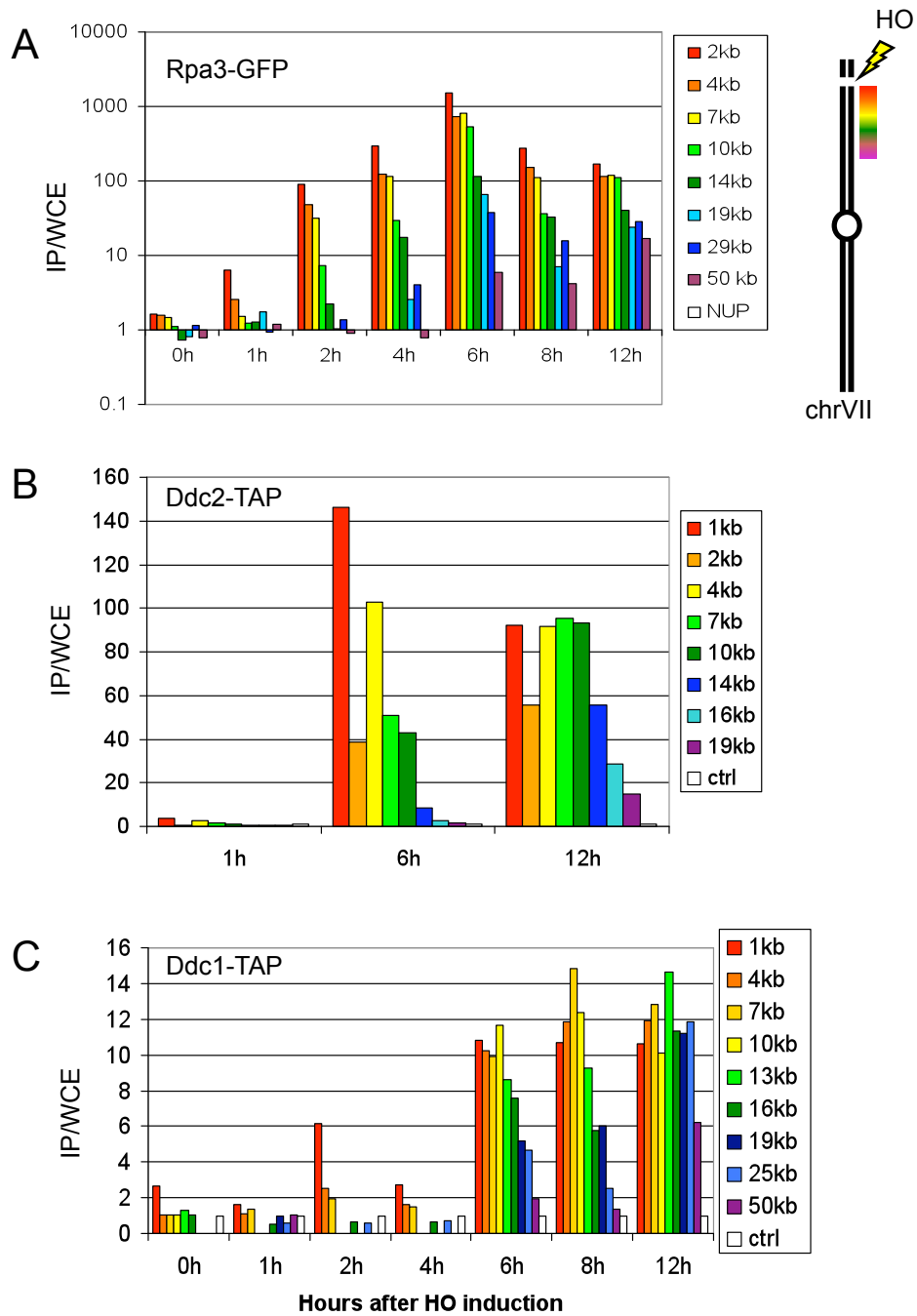
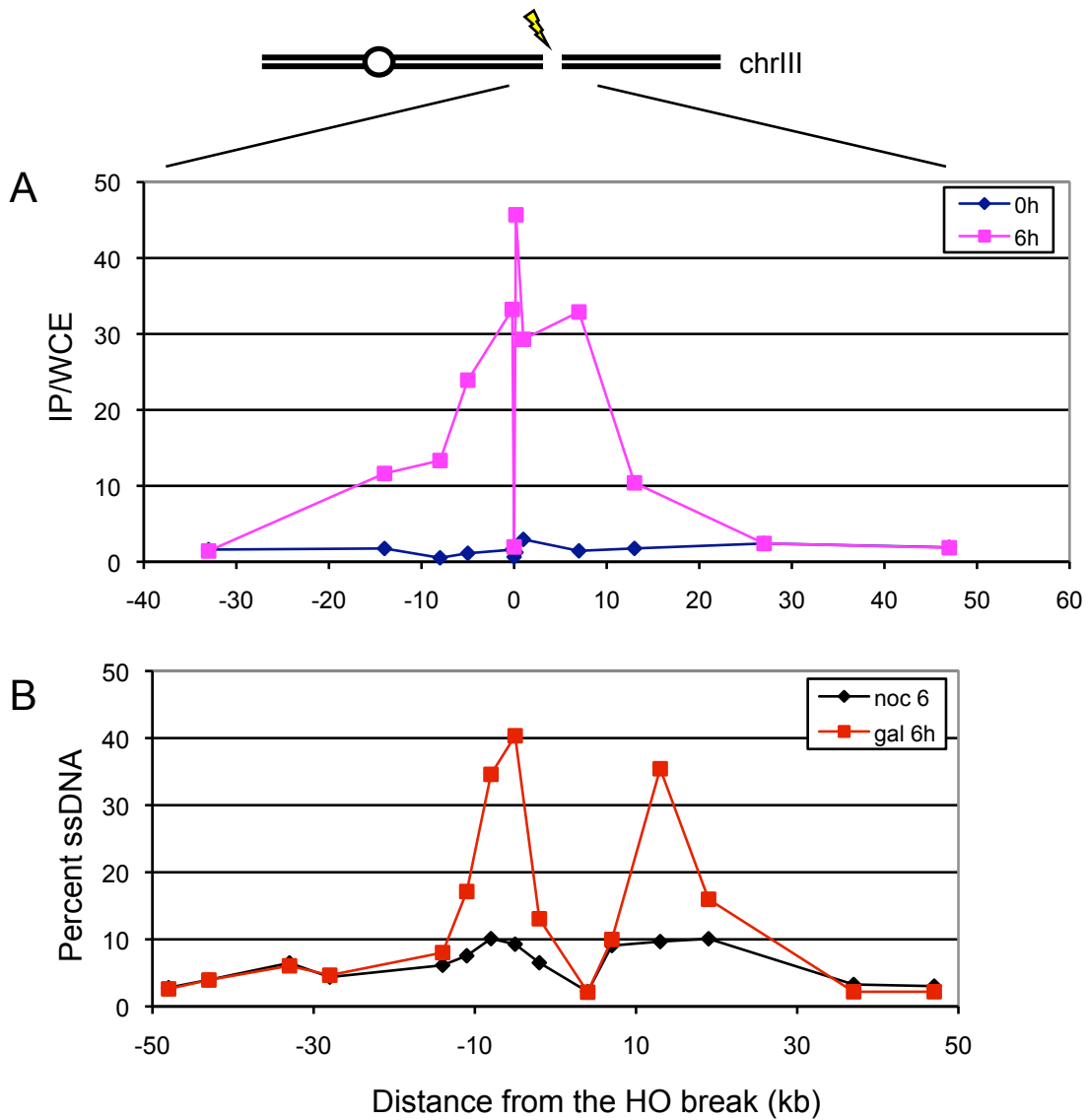


Figure 5. Ddc1 localization coincides with ssDNA proximal to a DSB. (A) Ddc1-TAP was immunoprecipitated for ChIP analysis in a strain utilizing the endogenous HO recognition site on chrIII. Extracts are collected at 0h or 6h after *GAL-HO* induction. (B) Genomic DNA was prepared from cells that have been treated for 6 hours with nocodazole or galactose to induce HO expression. Percent ssDNA was determined by the ratio of QPCR products from TaqI-cut genomic DNA to total DNA.



Chapter 4

Learning to adapt:

Suppression of the DNA damage checkpoint

by the *Saccharomyces cerevisiae* polo-like kinase, *CDC5*,

to promote adaptation

Title

CDC5 inhibits the hyperphosphorylation of the checkpoint protein Rad53, leading to checkpoint adaptation

Authors/Affiliations

Genevieve M. Vidanes¹, Frederic Sweeney², Sarah Galicia², Stephanie Cheung¹, Daniel Durocher², and David P. Toczyski^{1,*}

¹Department of Biochemistry and Biophysics

University of California San Francisco

2340 Sutter Street, San Francisco

CA 94115, USA

²Centre for Systems Biology

Samuel Lunenfeld Research Institute

Mount Sinai Hospital

600 University Avenue

Toronto, Ontario, M5G 1X5

Canada

Corresponding Author

*tozyski@cc.ucsf.edu

Abstract

The *Saccharomyces cerevisiae* polo-like kinase *CDC5* promotes adaptation to the DNA damage checkpoint, in addition to its numerous roles in mitotic progression. The process of adaptation occurs when cells are presented with persistent or irreparable DNA damage and eventually override the cell cycle arrest imposed by the DNA damage checkpoint. However, the mechanism of adaptation is unknown. We found that *CDC5* is dose-dependent for adaptation and its overexpression promotes faster adaptation, indicating that high levels of Cdc5 block the ability of the checkpoint to inhibit the downstream cell cycle machinery. To pinpoint the step in the checkpoint pathway at which Cdc5 acts, we overexpressed *CDC5* from the *GALI* promoter in damaged cells and examined each step in checkpoint activation individually. Cdc5 overproduction appeared to have little effect on the early steps leading to Rad53 activation. The checkpoint sensors, Ddc1 (a member of the 9-1-1 complex) and Ddc2 (a member of the Ddc2/Mec1 complex), properly localized to damage sites. Mec1 appeared active, since the Rad9 adaptor retained its Mec1 phosphorylation. Moreover, the damage-induced interaction between phosphorylated Rad9 and Rad53 remained intact. However, Rad53 hyperphosphorylation is mostly eliminated. Interestingly, although Rad53 no longer shows the strong electrophoretic shift associated with its *in vivo* autophosphorylation, it is still active in *in situ* phosphorylation assays, suggesting that Rad53, like Rad9, is still Mec1-primed. This is a unique situation that implies that overexpression of Cdc5 affects the cell in such a way that the Rad53 protein is primed and bound to its adaptor Rad9, but is unable to undergo autophosphorylation.

Author Summary

Surveillance mechanisms, termed checkpoints, have evolved to recognize the presence of DNA damage, halt cell division, and promote repair. The purpose of these checkpoints, ultimately, is to prevent the next generation of cells from inheriting a damaged genome. However, after futile attempts at repair over several hours of growth arrest, yeast cells eventually adapt and continue with cell division despite having persistent DNA lesions. This process of adaptation utilizes *CDC5*, a kinase that also has essential roles in promoting cell division. We found that increasing levels of *CDC5* promotes adaptation by suppressing the DNA damage checkpoint to relieve the cell division arrest. It is possible that cancer development may invoke a similar survival mechanism. *PLK1*, the human homolog of *CDC5*, has been reported to be overexpressed in various tumor types and been linked to poor prognosis. Understanding the mechanism of adaptation in yeast may provide valuable insight into the role of *PLK1* overexpression in tumor progression.

Introduction

Both exogenous pressures and normal cellular processes place stresses on the genome that commonly result in DNA lesions, such as DNA adducts, nicks, and breaks. A robust checkpoint response has evolved to quickly respond to the presence of damaged DNA. When triggered, this evolutionarily conserved checkpoint arrests the cell cycle and promotes repair to maintain the integrity of the genome for the next generation of cells. An inability to appropriately repair DNA can lead to mutations, loss of genetic information, or genomic instability.

Checkpoint activation begins with the recruitment of checkpoint sensors to the site of DNA damage. When a double-strand DNA break (DSB) occurs, the DNA ends are resected in a 5' to 3' direction by exonucleases, exposing stretches of single-stranded DNA (ssDNA) [62] [62,63]. The *Saccharomyces cerevisiae* checkpoint sensor complexes, which include the checkpoint clamp and the Mec1/Tel1 kinases, recognize the exposed ssDNA and accumulate at the break site [2,3,5,14]. The checkpoint clamp is a ring-shaped heterotrimeric complex that consists of Ddc1, Mec3, and Rad17 (referred to as the 9-1-1 complex) and is reminiscent of the well-studied replication processivity factor PCNA. The 9-1-1 clamp is likely loaded onto DNA at ssDNA-dsDNA junctions that are created by resection, in a manner similar to PCNA loading at replication sites [4,51,53,64]. Tel1 accumulates at DSBs and contributes to checkpoint activation [14], but works somewhat redundantly with major yeast kinase Mec1 [65], in contrast to the major role of its mammalian homolog [1]. The Mec1-binding partner, Ddc2, mediates the association with ssDNA by interacting with the ssDNA-binding protein RPA.

Similarly, the homologous mammalian kinase, ATR, and its interacting partner, ATRIP, localize to DNA damage via RPA [5].

The co-localization of the checkpoint sensors leads to the activation of the downstream effector kinases mediated by checkpoint adaptors [66,67]. Replication damage utilizes the Mrc1 (Claspin) adaptor to effect checkpoint signaling, whereas damage incurred outside of replication uses the Rad9 adaptor [68]. Upon damage, Rad9 is phosphorylated by Mec1, oligomerizes, and serves as a scaffold to promote the activation the effector kinases, Chk1 and Rad53 (Chk2 in mammals) [69,70,71,72,73,74]. Rad9 then mediates a priming Mec1-phosphorylation of Rad53 as well as subsequent auto-phosphorylation of activated Rad53 [73]. In *S. pombe*, the phosphorylation on Cds1 mediated by the Mec1 homolog Rad3, promotes a dimerizing interaction that helps promote Cds1 hyperphosphorylation[75].

If unable to repair genomic damage, yeast will eventually overcome the checkpoint and continue with cell division despite the persistence of a break, a process called adaptation. The *S. cerevisiae* polo-like kinase, Cdc5, was implicated to have a role in adaptation when the *cdc5-ad* allele was discovered in a screen for adaptation-defective mutants [76]. In addition, the timing of adaptation onset correlated with the loss of Rad53 activity [77] suggesting adaptation is a consequence of checkpoint inhibition mediated by Cdc5. Studies in higher eukaryotes provide supporting evidence that the polo-like kinase can inhibit the checkpoint response after damage. The *Xenopus* homolog of Cdc5, Plx1, decreases Chk1 activity by promoting the dissociation of the replication-checkpoint adaptor Claspin from chromatin [78]. Similarly, during recovery after DNA damage, the human Plk1 phosphorylates Claspin to promote its SCF^{βTrCP}-

dependent degradation, which in turn prevents further Chk1 activation [79,80,81].

In this study, we overexpressed *CDC5* from the GAL1 promoter to probe how Cdc5 interacts with the DNA damage checkpoint and to gauge its role in adaptation. We found that the checkpoint steps leading to Rad53 activation including checkpoint sensor localization, Mec1-phosphorylation of Rad9, and Rad9-Rad53 binding remained mostly unaffected by Cdc5 overproduction. However, damage-induced hyperphosphorylation of Rad53 was lost, likely due to an inability to autophosphorylate *in vivo*. We also found that Cdc5 and Rad53 interact both *in vivo* and *in vitro* and Cdc5 can phosphorylate Rad53 *in vitro*.

Results

***CDC5* is dose dependent for adaptation**

An allele of *CDC5*, *cdc5-ad*, was originally identified in a screen for adaptation-defective mutants [76]. To determine if the process of adaptation is sensitive to the dosage of *CDC5*, we first analyzed diploid yeast carrying various combinations of *CDC5* alleles: wildtype, *cdc5-ad*, or a deletion. The percentage of cells able to adapt to the DNA damage checkpoint was first measured by creating telomeric damage using the *cdc13-1* mutation. Shifting *cdc13-1* strains to the non-permissive temperature, destabilizes telomeres, causes the accumulation of ssDNA, thus eliciting a checkpoint response. We assayed adaptation by shifting these strains to the non-permissive temperature of 32°C for two hours, plating cells to prewarmed plates, and then counting the number of cells able to form a microcolony on a plate [82]. As expected, we found

that greater than 90% of *CDC5/CDC5* homozygous diploids were able to adapt after 10 hours of persistent DNA damage (Fig. 1A). Moreover, diploids that express *cdc5-ad* as the only functional *CDC5* allele (*cdc5-ad/cdc5-ad* and *cdc5-ad/cdc5Δ*) were unable to adapt for the duration of the 25-hour time-course. However, in heterozygous strains carrying only one copy of wild type *CDC5* (in combination with the *cdc5Δ* or *cdc5-ad* allele), the rate of adaptation slows and the number of cells that adapt drops to less than 50%. The slowed rate of adaptation is consistent with the idea that *CDC5* is dose dependent for adaptation. However, the drop in the total number of cells that adapt likely reflects the decreasing ability of diploids to survive after prolonged cell cycle arrest. Even arrests that are not associated with viability loss in the short term, such as those induced with temperature-sensitive alleles of the Anaphase Promoting Complex (APC) show loss of viability after about 10 hours, around the time that wildtype cells grown in glucose adapt. The observation that a *CDC5/cdc5Δ* strain shows a more significant defect than a *CDC5/cdc5-ad* diploid suggests that the *cdc5-ad* is not functioning as a gain of function mutation. If *cdc5-ad* had 50% activity for adaptation, the *cdc5-ad/cdc5-ad* and *CDC5/cdc5Δ* strains would have an identical capacity to support adaptation. Yet, the observation that a *cdc5-ad/cdc5-ad* strain showed a much more pronounced phenotype than a *CDC5/cdc5Δ* suggests that the *cdc5-ad* allele is very significantly impaired for *CDC5*'s adaptation activity.

To further investigate if increased levels of *CDC5* can promote adaptation, we analyzed haploid yeast expressing endogenous *CDC5* with or without additional copies of galactose inducible *CDC5*. Greater than 80% of wildtype haploid cells adapted by 12 hours (Figure 1B). This is slightly later than seen in the previously described experiment,

likely because these cells are grown in a poorer carbon source. Thus, as seen previously, overexpression of Cdc5 causes re-budding of checkpoint arrested cells [71].

***CDC5* suppresses the DNA damage checkpoint**

Pelliccioli *et al.* [77] provided evidence that the timing of adaptation coincides with a loss of Rad53 hyperphosphorylation. In contrast, the adaptation-defective allele, *cdc5-ad*, remains arrested with an activated checkpoint. These data suggest that an as yet unidentified step in the DNA damage checkpoint is turned off to allow cells to adapt. However, adaptation is a long and asynchronous process, making studying the molecular mechanism difficult. Moreover, several pathways may impinge upon the checkpoint to promote adaptation. We used the overexpression of *CDC5* as a tool to probe specifically how *CDC5* impinges on the DNA damage checkpoint. We first wanted to determine whether the overexpression of *CDC5* inhibited the checkpoint pathway itself, or promoted cell cycle progression non-specifically at a step downstream of the checkpoint. Damage was induced by shifting *cdc13-1* cultures to the non-permissive temperature of 32°C for 2 hours, leading to Rad53 phosphorylation. *CDC5* was then induced by adding 2% galactose to strains expressing *CDC5* under the *GAL1* promoter. Nocodazole was added simultaneously with galactose to prevent the adapting cells from re-entering the cell cycle. After galactose addition, the phosphorylation of Rad53 dropped significantly in strains harboring the *GAL-CDC5* construct, but not in control strains lacking the construct (Figure 1D). This suppression of the checkpoint was not specific to *cdc13-1*-induced damage. Rad53 phosphorylation also dropped when the DSB-inducing drug

zeocin was used (Figure 1E), supporting the notion that *CDC5* promotes checkpoint inactivation.

Recruitment of checkpoint sensors to DSBs is unaffected by *CDC5* overexpression

To determine how *CDC5* suppresses Rad53 phosphorylation, we examined each of the upstream steps leading to Rad53 activation after *CDC5* overexpression.

Recruitment of checkpoint sensors to DSBs is one of the earliest events in checkpoint activation (Figure 1B) and can be visualized by microscopy [3,14]. Therefore, we monitored the localization of GFP fusions to the checkpoint sensors Ddc1 and Ddc2, a 9-1-1 checkpoint clamp subunit and the Mec1 binding partner, respectively. Cells were treated with zeocin for two hours before adding galactose to induce *CDC5* for an additional two hours, as in Figure 1E, and were then examined by fluorescence microscopy. Both Ddc1-GFP and Ddc2-GFP form multiple foci in cells treated for four hours with zeocin (Figure 2A, left column). Interestingly, *CDC5* induction during the second half of the zeocin treatment did not produce an observable change in either Ddc1-GFP or Ddc2-GFP foci formation (Figure 2A, right column) in contrast to its effect on Rad53 phosphorylation at 4 hours (Figure 1E, lanes 4 and 9). The maintenance of checkpoint sensor localization to break sites, despite *CDC5* overexpression, suggests *Cdc5* likely acts downstream of this recruitment step, such that despite continued localization of these proteins to the DSB, signaling is eliminated. Previous experiments had shown that at late timepoints, Ddc2-GFP foci were lost in a subset of adapted cells [3]. These results suggest that this may not be the result of *Cdc5* activity, although it may contribute to adaptation.

Regulation of the Rad9 checkpoint adaptor in damage remains unaffected by *CDC5*

We next investigated if Cdc5 lowers Rad53 phosphorylation by interfering with the Rad9 checkpoint adaptor. Rad53 activation occurs through the coordination of the adaptor Rad9 and the sensor kinase Mec1 (Figure 1C). Following checkpoint recruitment to DSBs, Rad9 is phosphorylated by Mec1 and, to a lesser extent, Tel1. This phosphorylation promotes Rad9 association with Rad53[69,70,74]. DNA damage-induced Mec1/Tel1 phosphorylation causes a substantial electrophoretic mobility shift in Rad9. This step in checkpoint activation was also largely unchanged by the induction of *CDC5* (Figure 2B, top). To verify that the observed shift in Rad9 was due to phosphorylation by Mec1/Tel1, we probed immunoprecipitated Rad9 with a phospho-specific antibody that recognizes glutamine directed phospho-serine and phospho-threonine residues, which correspond to Mec1 phosphorylation motifs. As expected, the pS/pT-Q antibody only recognized Rad9 after damage induction and with increasing intensity over time (Figure 2B). Similar to the Rad9-FLAG Western, *CDC5* overexpression resulted in only a subtle change in the electrophoretic mobility shift. This two-fold drop in Rad9 hyperphosphorylation was seen at the last (5 hr) timepoint, but was not significant at the 4 hour timepoint, despite the fact that Rad53 phosphorylation was already lost by this time (Figure 2B). Thus, we conclude that Mec1/Tel1 are able to recognize and phosphorylate Rad9 properly despite *CDC5* induction, suggesting that their kinase activity is not affected.

Cdc5 could disrupt Rad9 function without blocking Mec1/Tel1 phosphorylation of Rad9. First, we determined whether Rad53 remained associated with Rad9 after

CDC5 overexpression. We immunoprecipitated FLAG-tagged Rad9 in the presence of DNA damage with, or without, overexpression of *CDC5* (Figure 2B, bottom). As previously reported, Rad53 co-immunoprecipitated with Rad9 after induction of DNA damage. Despite the fact that *CDC5* overexpression eliminated Rad53 hyperphosphorylation, Rad53 still associated with Rad9. The reciprocal experiment in which we immunoprecipitated Rad53 showed that only shifted Rad9 binds Rad53. Again, *CDC5* overexpression only had a marginal effect on Mec1/Tel1 dependent phosphorylation of Rad9 and had no effect on Rad9's ability to interact with Rad53, despite Rad53's hypophosphorylated state (Figure 2C). Next, we examined the oligomeric state of Rad9. Rad9 has been shown to form a homodimer through its C-terminal BRCT-containing tail. It is possible that *CDC5* could disrupt this higher order structure, thus disabling Rad9's ability to promote Rad53 activation. To determine whether Rad9 multimerization was affected by *CDC5* over expression, we expressed two differently epitope-tagged alleles of Rad9. Overexpression of *CDC5* did not affect the efficiency with which we were able to co-immunoprecipitate myc-tagged Rad9 with FLAG-tagged Rad9 (Supplemental Figure 1). Together, these data suggest that high levels of Cdc5 specifically block the ability of Rad9 to promote Rad53 auto-phosphorylation without affecting the make-up of the Rad9-Rad53 complex.

Cdc5 kinase activity is required to suppress Rad53 hyperphosphorylation.

To determine whether the loss of Rad53 hyperphosphorylation requires Cdc5 kinase activity, we compared the effects of overexpressing *CDC5* and the kinase-defective allele *cdc5-K110A*. Increasing levels of *CDC5* after checkpoint activation

resulted in a decrease in Rad53 phosphorylation, as expected (Figure 3A). In contrast, inducing *cdc5-K110A* had no effect (Figure 3A) suggesting Cdc5's catalytic activity is necessary for its ability to inactivate checkpoint signaling. Interestingly, induction of the *cdc5-ad* allele produced an intermediate effect, manifest by the later and less robust decrease in Rad53 phosphorylation compared to *CDC5* induction (Figure 3A, lanes 13-16 and 5-8), consistent with its reduced ability to promote checkpoint adaptation.

Cdc5 downregulates the damage checkpoint independently of the Ptc2, Ptc3, and Cdc14 phosphatases.

The PP2C-type phosphatases, Ptc2 and Ptc3, have been implicated to have roles in adaptation and in regulating Rad53 phosphorylation [83,84]. We generated *ptc2Δ ptc3Δ* strains to test the possibility that *CDC5* acts indirectly on the checkpoint via these phosphatases. If this were true, we would expect the *ptc2Δ ptc3Δ* strains to be resistant to *CDC5* overexpression. We instead found the damage-induced Rad53 phosphorylation was reduced by *CDC5* induction even in the absence of the Ptc2 and Ptc3 phosphatases (Figure 3B), implying *CDC5* works independently of these phosphatases. We cannot, however, rule out the possibility that Cdc5 functions by activating other phosphatases that could mediate the loss of Rad53 phosphorylation.

One of the key roles of the Cdc5 kinase is to advance anaphase by promoting the release of the Cdc14 phosphatase from the nucleolus, which in turn dephosphorylates CDK substrates. It has been reported that overexpression of *CDC5* results in the premature release of the Cdc14 [85]. Previous work has suggested a role for CDK in checkpoint signaling, in part through its regulation of processing of the DNA damage site

[15,86,87]. Subsequent work indicated that this was in part through Rad9. CDK phosphorylation of Rad9 was shown to be important for full checkpoint signaling, but not absolutely vital to initiate Rad53 phosphorylation [66]. To explore the possibility that the loss of Rad53 phosphorylation was a secondary effect of Cdc14 release, we compared the effect of galactose-induced overexpression of *CDC5* and *CDC14* on checkpoint signaling. Unlike *CDC5* overexpression, *CDC14* overexpression had little observable effect on damage-induced Rad53 phosphorylation (Figure 3C). However, induction of both *CDC5* and *CDC14* produced the same subtle change in the Rad9 phospho-shift and twofold loss of recognition by the pS/pT-Q antibody (Figures 2B, 2C, and 3C). Neither *CDC5* nor *CDC14* overexpression disrupts the damage-dependent interaction between Rad9 and Rad53 (Figure 3C). Lastly, the *in situ* assay (ISA) revealed that Rad53 activity remained high despite *CDC14* overexpression (Figure 3C, bottom). Together, these results suggest that checkpoint inhibition by Cdc5 is not solely due to Cdc14 activation.

We next determined whether Rad53, like Rad9, retained its Mec1-priming phosphorylation upon Cdc5 overexpression. Given that Rad53 always remained a subtle doublet after Cdc5 overexpression (e.g. see Fig. 1D and 2B) and that Mec1 appeared to retain its activity as judged by Rad9 phosphorylation, we expected that the Mec1-priming phosphorylation on Rad53 was intact. Extensive efforts to examine this using the phospho-S/T Q antibodies were unsuccessful, even on Rad53 purified from damage-only control cells. We instead performed an *in situ* assay (ISA), which measures autophosphorylation by incorporation of [γ -³²P]ATP to membrane-bound renatured Rad53 [88]. By ISA, we observed that Rad53 appeared to retain its kinase activity, despite the fact that it lost hyperphosphorylation *in vivo* (Figures 3C and 4A). Previous experiments

on the *S. pombe* homolog of Rad53, Cds1, have shown that priming phosphorylation by the Mec1 homolog promotes Cds1 dimerization and subsequent autophosphorylation [75]. Thus, this result provides a unique (to our knowledge) situation in which Rad53 is Rad9 bound and primed to become hyperphosphorylated, but rather remains hypophosphorylated *in vivo*.

Cdc5 binds and phosphorylates Rad53.

Polo-like kinases recognize substrates that have been previously phosphorylated by other kinases, such as CDK and ATM/ATR in higher eukaryotes [78,79,80,81,89]. Rad53, phosphorylated by the CDK and Mec1/Tel1 kinases [65,66,90], therefore is a reasonable candidate substrate for Cdc5. Alternatively, Rad53 contains two forkhead-associated (FHA) domains that are important for checkpoint function [70], and mediate association with phosphorylated proteins, such as Rad9 [91] and potentially Cdc5.

We first examined if Cdc5 was also able to interact with Rad53 *in vivo*. In fact, the human homolog of Rad53, Chk2, has been reported to bind directly with the human Plk1 [92,93] (T and Stern). HA-Cdc5, as well as the kinase dead HA-cdc5-K110A, were indeed found to immunoprecipitate with Rad53 (Figure 4B, lanes 1-8 and data not shown) and not come down in a control immunoprecipitations performed in a *rad53Δ* strain (Supplemental Figure 2). To ensure the interaction of Rad53 and Cdc5 during an active DNA damage checkpoint is not mediated by the Rad9 adaptor protein, we also performed the co-immunoprecipitation in a *rad9Δ* strain. HA-Cdc5 was still co-immunoprecipitated with Rad53 in the absence of Rad9 (Figure 4B, lanes 9-12), suggesting the binding between Cdc5 and Rad53 is direct. The *in vivo* interaction between Rad53 and Cdc5 was

also found to occur independently of damage (Figure 4B, lanes 13-16), which is consistent with both the Rad9-independent binding data (Figure 4B, lanes 9-12) and the human Chk2-Plk1 interaction data [92,93].

Having discovered that the Cdc5 kinase activity is critical for its function to reduce Rad53 phosphorylation, we performed *in vitro* kinase assays to determine if Rad53 could be a direct substrate of Cdc5. The HA-Cdc5 kinase was isolated from yeast extracts that were either untreated or damaged with zeocin. To ensure that the *in vitro* phosphorylation of Rad53 was specific to Cdc5 kinase activity and not a product of Rad53 autophosphorylation, all Rad53 substrates harbored the D339A kinase inactivating mutation. This Rad53-D339A substrate was either otherwise wildtype or also carried additional mutations in one or both of the FHA domains. The rad53 R70A mutation corresponds to the N-terminal FHA1 domain and the R605A mutation to the C-terminal FHA2 domain. Similar to the *in vivo* binding data, the *in vitro* phosphorylation of Rad53 by Cdc5 can occur independently of the DNA damage. HA-Cdc5, isolated either from untreated extracts (Figure 4C) or DNA damaged extracts (Figure 4D), clearly phosphorylated Rad53 *in vitro*, as seen by both the incorporation of radiolabelled phosphate or the Cdc5-induced electrophoretic shift of Rad53. As expected, this result required a functional HA-Cdc5 since no Rad53 phosphorylation was observed when the kinase dead mutant, HA-cdc5-K110A, was used as a control (Supplemental Figure 3). The rad53 R605A mutant seemed to be phosphorylated to a similar level as the wildtype. Surprisingly, the rad53 R70A mutant alone was barely phosphorylated and the R70A R605A double mutant was not at all phosphorylated by Cdc5 (Figures 4C and 4D).

These data suggest that the Rad53 FHA1 phosphobinding domain (and to a lesser extent the FHA2 domain) promote Cdc5's ability to phosphorylate Rad53.

To test the model that Cdc5 targeting of Rad53 to promote adaptation is mediated by the Rad53 FHA1 domain, we compared the phenotypes of *CDC5*, *cdc5-ad*, and *rad53-R70A* in an adaptation assay. The *rad53 R70A R605A* double mutant is checkpoint defective and thus precludes our ability to measure an adaptation phenotype [73,94]. In contrast, the Rad53-R70A allele has only a mild negative effect on checkpoint activation. If Cdc5 promoted adaptation by directly phosphorylating Rad53 in a FHA1-dependent manner, the *rad53 R70A* mutant would display an adaptation defect similar to *cdc5-ad* allele *in vivo*. After 6 hours in damage, greater than 85% of both *cdc5-ad* and *RAD53* strains were arrested with one to two cells per microcolony, whereas 80% of *rad53-R70A* had progressed to three to four cells per microcolony (Figure 4E). While the *rad53-R70A* mutant was able to establish checkpoint signaling and arrest [73,94], it was unable to maintain as extended a checkpoint arrest as a wildtype *RAD53* (Figure 4E) and thus prevented us from making any conclusions about its ability to adapt to damage. In addition, overexpression of *HA-CDC5* further lessened the phosphorylation observed in the *rad53 R70A* mutant, suggesting that the Cdc5-FHA1 interaction was not vital to our observed inhibition of the checkpoint by Cdc5 (Supplemental Figure 4A). However, we were unable to rule out the possibility that the redundancy seen for the two FHA domains was more significant *in vivo*.

The Rad53 FHA1 and FHA2 domains recognize the pT-x-x-D and pT-x-x-(I/L) motifs, respectively [89,95]. To circumvent the checkpoint defect of the Rad53 FHA mutants, we created mutations in Cdc5 to residues that have been reported to be

phosphorylated *in vivo* [96] and loosely match the Rad53 FHA binding motifs. The candidate Cdc5 sequences 29-pT-A-D-L and 70-pT-P-P-pS were mutated to create *HA-cdc5-T29A T70A S73A*. We found however, that galactose-induced overexpression of the *HA-cdc5-T29A T70A S73A* mutant was still able to suppress Rad53 phosphorylation to the same degree as *HA-CDC5*, unlike *HA-cdc5-ad* which produced a delayed effect (data not shown).

Discussion

Polo-like kinases participate in several processes that collectively promote mitotic progression, including mitotic exit, early anaphase, APC activation, and sister chromatid separation [97,98,99,100]. The discovery of an adaptation-defective allele of *CDC5* suggested that this kinase also had a role in negatively regulating the DNA damage checkpoint [76], however the mechanistic details were yet unknown. Here we show that Cdc5 does not inhibit formation of the Rad9-Rad53 complex, and yet somehow blocks the ability of the Mec1-primed Rad53 molecules to produce hyperphosphorylated Rad53 *in vivo*.

Adaptation to DNA damage begins to occur after approximately 6-8 hours of cell cycle arrest if cells were unable to repair the damage. Loss of checkpoint signaling has been previously shown to correlate with the onset of adaptation [77]. However, there could be multiple pathways converging on the checkpoint after an extended cell cycle arrest. One of the advantages of using *CDC5* overexpression is that it isolated *CDC5* specific effects and did not activate other pathways. For example, the Ptc2 and Ptc3

clearly have a role in Rad53 regulation and deletion of these phosphatases display an adaptation-defective phenotype [83]. However, we found that checkpoint suppression caused by *CDC5* overexpression occurred in the absence of both these phosphatases (Figure 3B), suggesting that at least two pathways work independently to promote adaptation. Rad53 has recently been proposed to act in a negative-feedback loop, in which Rad53 phosphorylates Rad9 to prevent the BRCT-SCD domain-specific oligomerization of Rad9 that is required to maintain checkpoint signaling [101]. While this negative-feedback loop may also feed into adaptation, our results showing overproduced Cdc5 prevents *in vivo* Rad53 autophosphorylation suggest Cdc5 exerts its effect upstream of this loop.

We found that Cdc5 and Rad53 could interact both *in vivo* and *in vitro*, which could support the notion that Cdc5 directly inhibits Rad53. Cdc5 kinase activity was required to suppress Rad53 phosphorylation, eliminating the mechanism of simple binding inhibition. Strangely, hypophosphorylated Rad53 from Cdc5 overproducing lysates retained its ability to trans-autophosphorylate by ISA (Figure 4B, lane 8), suggesting Rad53 was not inactivated *per se*. The ISA likely recapitulates Rad53 *in vivo* kinase activity, but not the physical interaction between the kinase and other Rad53 substrates. The fact that the ISA assay does not require Rad9 is consistent with this notion that Rad53 autophosphorylation can happen in the absence of Rad9 when Rad53 molecules are locally concentrated, whereas Rad9 is essential for Rad53 autophosphorylation *in vivo*.

Cdc5 was able to directly phosphorylate Rad53 *in vitro*. Cdc5 phosphorylation might affect the positioning of Rad53 in respect to either other Rad53 molecules or Rad9

so as to prevent proper Rad53 trans-autophosphorylation. The requirement for active and phosphorylated Rad53 to release from Rad9 [102], would suggest these Rad9-bound hypophosphorylated Rad53 molecules could act dominantly to prevent further checkpoint activation, as does expression of the dominant kinase-dead allele of *RAD53* [88].

Alternatively, Rad53 could bridge an interaction between Cdc5 and Rad9 and promote Cdc5 phosphorylation of Rad9 that could subsequently interfere with proper Rad53 autophosphorylation. The latter model has the benefit of targeting the checkpoint mediator responsible for activating the two parallel effector kinases Rad53 and Chk1, both shown to lose activity as cells adapt [77].

Our demonstration that Cdc5 phosphorylation of recombinant Rad53 depends on both Rad53 FHA domains (predominantly FHA1) (Figures 4C and 4D) is particularly intriguing. First, it suggests that this activity is quite specific. Moreover, it argues that Rad53 provides the binding specificity to allow Cdc5 to phosphorylate it, in contrast to the classic model in which polo-like kinases recognize a substrate via their phosphobinding polo-box domains and then subsequently phosphorylate the bound substrate [103] and is also different from how the human homologs, Chk2 and Plk1, are reported to interact [93]. If the Rad53 FHA domains indeed mediate a *bona fide* interaction between Rad53 and Cdc5 critical for adaptation, we expected FHA mutants to display an adaptation defect. However, our attempts to gauge adaptation phenotypes in FHA mutants were complicated by the necessity that adaptation-defective mutants must also be checkpoint proficient. Mutation of key arginine residues that coordinate phosphothreonine binding in Rad53 FHA1 (R70) and FHA2 (R605) domains to alanine results in a checkpoint null phenotype similar to that of a *rad53Δ* [73,94,104], thus

preventing us from examining the double mutant. The partial checkpoint phenotype we observed with the *rad53-R70A* (FHA1) mutant can be attributed to the fact that both the Rad53 FHA domains interact with phosphorylated Rad9 and loss of FHA1 binding can be mostly but not completely compensated by FHA2 [91,94,105,106]. While we could not adequately measure an adaptation defect in the FHA1 mutant, overexpression of *CDC5* was able to decrease the damage-dependent phosphorylation of *rad53-R70A*, suggesting the mutation of the FHA1 domain alone is insufficient to prevent *CDC5*'s *in vivo* ability to block Rad53 hyperphosphorylation. Yet, the possibility remains that both FHA domains are redundant for this function.

Cdc5 can now be added to the growing list of proteins that interact with the Rad53 FHA1 domain. Rad53 contains two FHA domains, one at each terminus, whereas homologous proteins such as human Chk2 and *S. pombe* Cds1 contain only one N-terminal FHA domain. Although both Rad53 FHA domains contribute to its checkpoint function, the N-terminal FHA1 is more structurally similar to its homologous counterparts. This raises interesting prospects on how Rad53's FHA1 domain facilitates interactions with downstream targets including Dbf4, Asf1, Mdt1, Rad9, and other Rad53 molecules [70,95,104,107,108], as well as promote its own inactivation by interacting with Ptc2 [83,84] and Cdc5. Perhaps, the specificity conferred by Rad53's FHA1 domain may depend on the biological availability of its substrates, determined by their phosphorylation status, degree of affinity, or localization.

Our results strongly suggest the polo-like kinase, Cdc5, can inhibit checkpoint signaling at the level of Rad53 regulation. The step of effector kinase activation is a point in the checkpoint-signaling cascade that provides both a threshold of Rad53

hyperphosphorylation to prevent premature or unnecessary checkpoint activation as well as an amplification step in which primed Rad53 can activate additional Rad53 molecules in a positive feedback loop. The findings that both the *in vivo* interaction and the *in vitro* phosphorylation of Rad53 by Cdc5 imply that there is potential for a constitutive interaction, in agreement with human Chk2 and Plk1 data [93]. While the biological significance for a constitutive interaction is not yet clear, it presents the opportunity for each kinase to inhibit the other, to generate a switch-like decision to undergo adaptation. This leads us to question what can tip the balance of this potential inhibitory face-off: the activity of a third kinase such as CDK on either or both Rad53 and Cdc5, or the relative strength of their interaction compared to other substrates?

Adaptation can be considered as a final attempt at survival after yeast have exhausted all other repair options. However, as a consequence of promoting cell division in the presence of DNA damage, adaptation also results in increased genomic stability [109]. Our study of adaptation, particularly our use of *CDC5* overexpression, may provide valuable insights into the mechanisms of tumorigenesis. *PLK1* been reported to be overexpressed in various tumors including non-small-cell lung cancer, melanoma, colorectal cancer, and Non-Hodgkin lymphoma. In addition, the levels of *PLK1* in a subset of tumor types may provide prognostic value [110,111]. Our work implies that, if indeed parallel with adaptation, *PLK1* overexpression could lead to checkpoint suppression, an enhanced rate of mutagenesis due to genomic instability, and ultimately carcinogenesis.

Materials and Methods

Adaptation assay. Adaptation can be assessed morphologically by counting the number of cells in a microcolony as previously described [82]. Arrested, large-budded cells are counted as two cells. Any additional budding beyond the two-cell stage is considered as adapted.

Rad53 and Rad9 Immunoprecipitation. Cells (OD=50) were collected for each immunoprecipitation (IP). The Rad53 IP was carried out with 1 μ l/IP of polyclonal DAB001 (gift from D. Durocher) on protein A Dynabeads (Invitrogen) as previously described [73]. For Rad9-FLAG purification, cells were subjected to glass bead lysis at 4°C in lysis buffer (25 mM HEPES-OH, pH7.5, 250mM NaCl, 0.2% Triton X100, 1mM EDTA, 10% glycerol, and protease inhibitor cocktail). 15 μ l of Sigma Anti-FLAG M2 agarose beads were added to each sample and allowed to incubate at 4°C for 2 hours. The beads were washed four times with lysis buffer. The beads were boiled in SDS-PAGE loading buffer to elute bound proteins.

Rad53 and Cdc5 Kinase Assays. The Rad53 ISA was performed as previously described [88]. Phosphorylation of Rad53 in the Cdc5 kinase assay was performed as previously described [73].

Plasmids and Reagents. D. Durocher kindly shared anti-Rad53 DAB001 as well as plasmids YCplac33-RAD53, YCplac33-rad53-R70A, YCplac33-rad53-R605A, and YCplac33-rad53-R70A R605A. To create *RAD53::TRP1* knock-in cassettes, the *TRP1*

gene was PCR amplified from pRS304 to introduce flanking *Sma*I restriction sites. The *Sma*I cut *TRP1* marker was blunt ligated into *Bsa*AI-digested YCplac33-*RAD53* to introduce *TRP1* ~800 bp upstream of the *RAD53* ORF to create pGMV18. The purified *Eco*RI fragment from pGMV18 was used as the *RAD53::TRP1* knock-in cassettes. To make *rad53-R70A::TRP1*, *rad53-R605A::TRP1* and *rad53-R70A R605A::TRP1* knock in cassettes, the *TRP1* marker was excised from pGMV18 with *Xcm*I and introduced into YCplac33-*rad53-R70A*, YCplac33-*rad53-R605A*, and YCplac33-*rad53-R70A R605A*, respectively, and the purified *Eco*RI fragment from the resulting plasmids were used in the yeast transformation. D. O. Morgan kindly provided the GAL-*HA3-CDC5*, GAL-*HA3-cdc5-ad*, and GAL-*HA3-cdc5-K110A* overexpressing plasmids. The pEM120 (GAL1-*CDC5-3xHA*) and derivative plasmids: pEM131 (*cdc5-T70A*), pEM138 (*cdc5-T29A*) were kind gifts from D. Kellogg. These plasmids were used to clone the *cdc5* mutants into the vectors provided by D.O. Morgan to create the following plasmids: pGMV14 (pRS306-GAL-3HA-*cdc5-T70A*), pGMV15 (pRS306-GAL-3HA-*cdc5-T29A*), and pGMV16 (pRS306-GAL-3HA-*cdc5-T29A T70A*). Quickchange mutagenesis was used to add the third S73A mutation to create pGMV22 (pRS306-GAL-3HA-*cdc5-T29A T70A S73A*). These plasmids were cut with *Nco*I for integration at the *ura3* locus.

Figure Legends

Figure 1. *CDC5* overexpression promotes adaptation by suppressing checkpoint signaling. (A) Adaptation was measured by microcolony assay in diploid strains carrying a combination of *CDC5*, *cdc5-ad*, or *cdc5Δ* alleles, or (B) in haploid strains with

or without additional copies of integrated GAL-HA-CDC5. (C) Schematic model of checkpoint signaling. (D) Rad53 was analyzed by Western blots from cells that did or did not overexpress *HA-CDC5* after DNA damage was induced by shifting to the non-permissive temperature of *cdc13-1* strains or (E) by treating cells with 3.3μg/ml zeocin. 2% galactose and 10μg/ml nocodazole were added after 2 hours of damage induction.

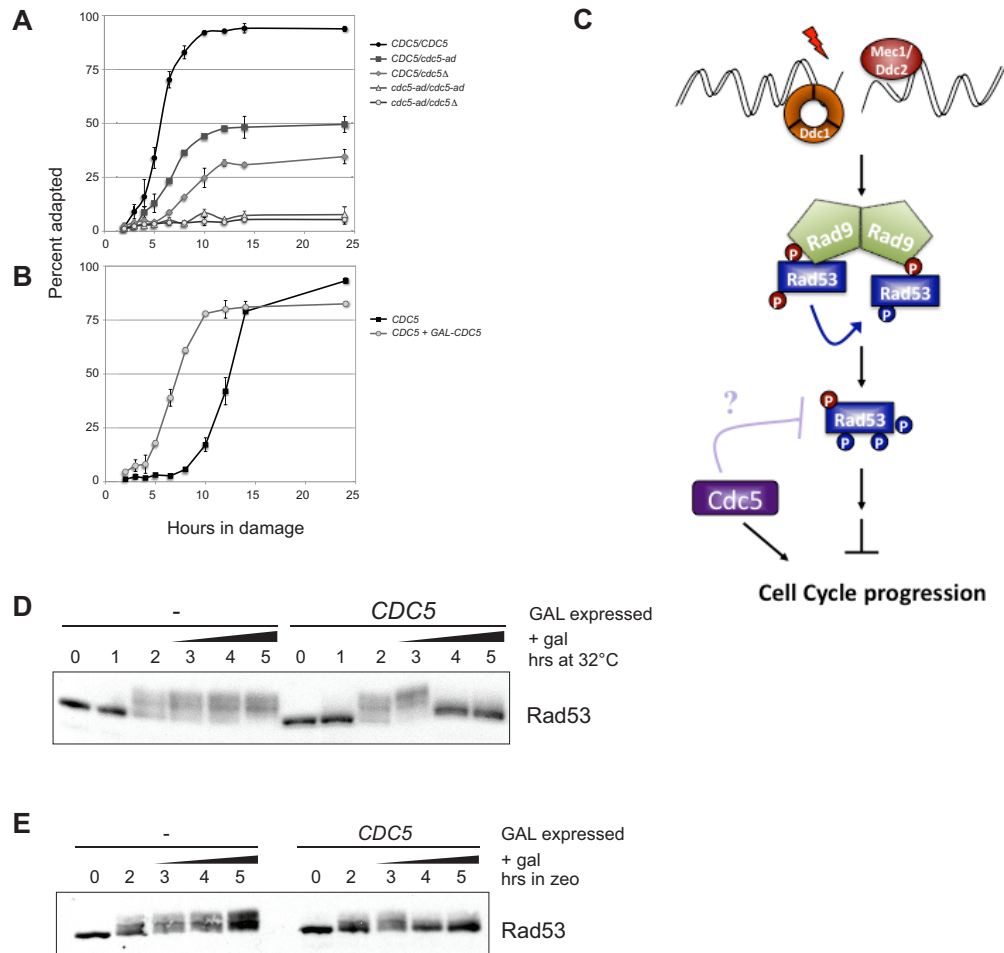


Figure 2. *CDC5* impinges on checkpoint signaling pathway at the step of Rad53

phosphorylation. (A) After 2 hours of 3.3 μ g/ml zeocin treatment, 10 μ g/ml nocodazole

and 2% galactose was added to induce blank or *HA-CDC5* for an additional 2 hours.

Cells were examined by fluorescence microscopy to visualize Ddc1-GFP or Ddc2-GFP

localization. (B) Cells were DNA damaged by shifting *cdc13-1* strains to 32°C for 2

hours then induced to express *HA-CDC5*. Rad9-FLAG was precipitated from lysates with

Sigma α -FLAG conjugated agarose beads. IP and lysates were analyzed by Western

blotting with the indicated antibodies. (C) The reciprocal IP was performed as described

in (B), immunoprecipitating Rad53 with the α -Rad53 (DAB001, from the Durocher lab)

antibody on Protein A Dynabeads. Strains listed as +/- damage are *cdc13-1* or *CDC13*,

respectively.

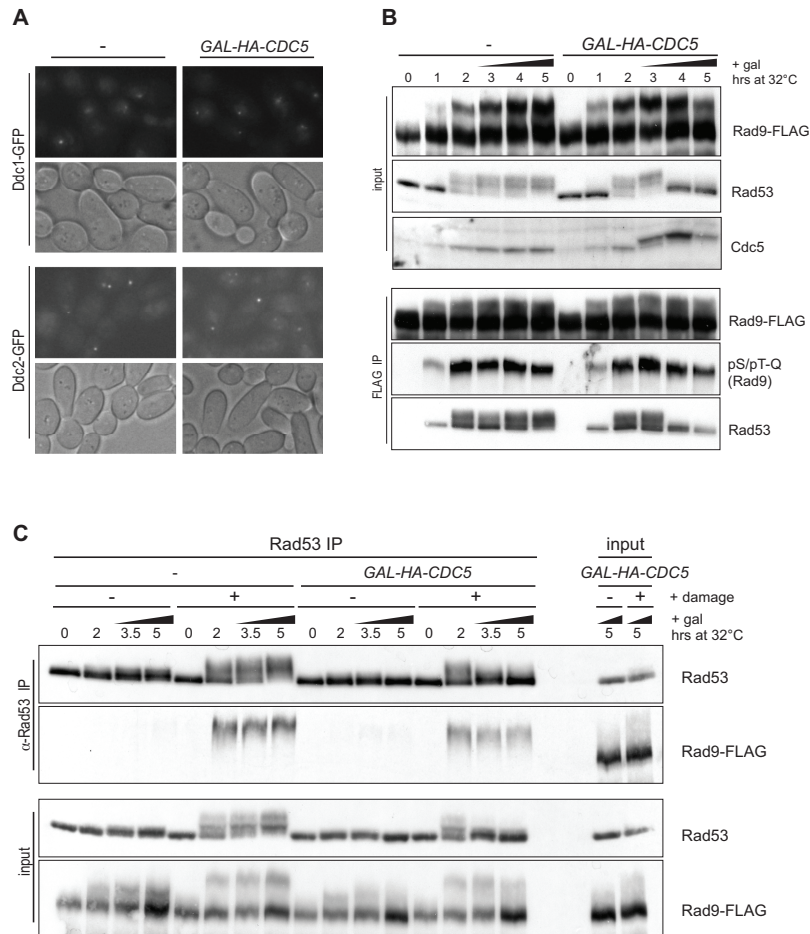


Figure 3. Suppression of Rad53 phosphorylation requires Cdc5 kinase activity but is independent of Ptc2, Ptc3, or Cdc14 phosphatases. Rad53 phosphorylation was examined by Western blot from cells that have been damaged for 2 hours before nocodazole and galactose was added to induce (A) *CDC5*, the kinase inactive *cdc5-K110A*, or adaptation defective *cdc5-ad* allele, (B) or *CDC5* in cells deleted for the *PTC2* and *PTC3* phosphatases. (C) Rad53 was immunoprecipitated with α -Rad53 from cells treated as above that express either *HA-CDC5* or *CDC14-Pk*. An additional *rad9 Δ* strain +/- *GAL-HA-CDC5* was examined as a control. Lysates and IP samples were analyzed by western blotting with the indicated antibodies.

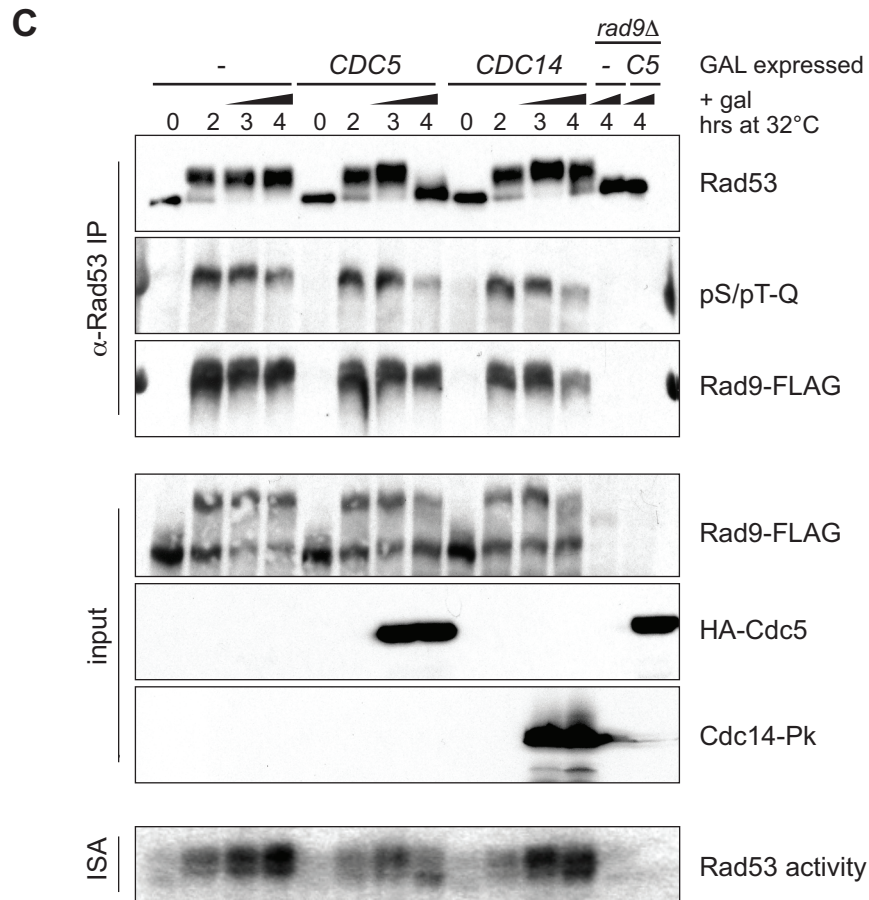
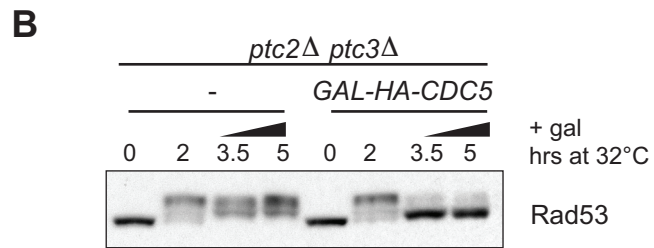
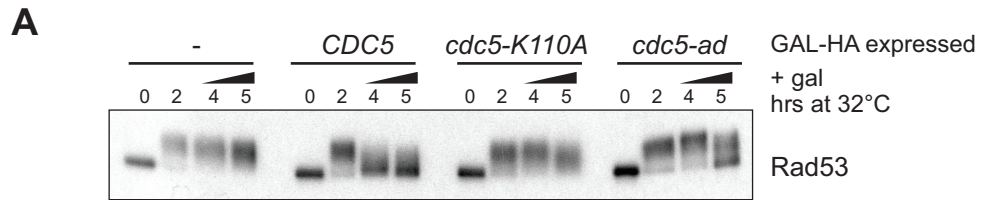
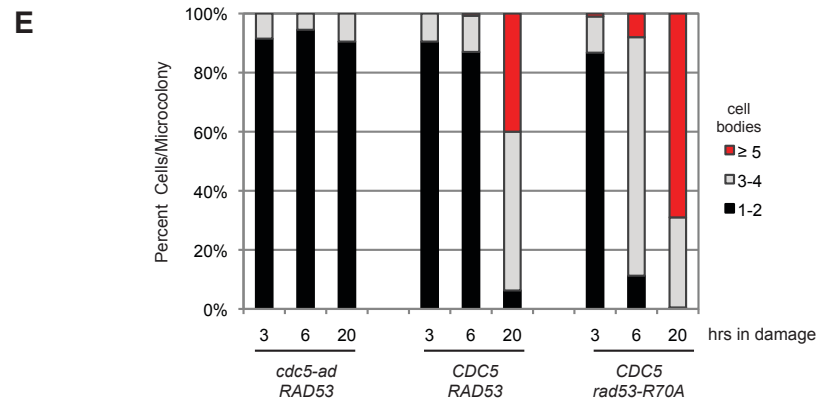
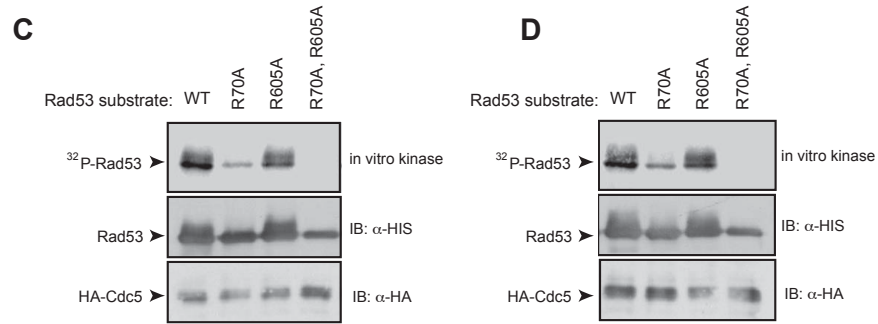
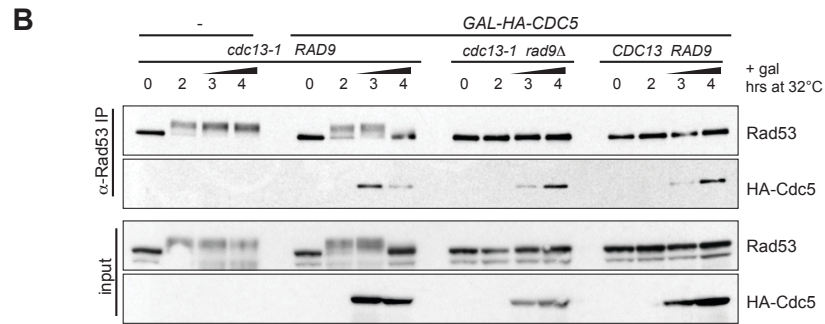
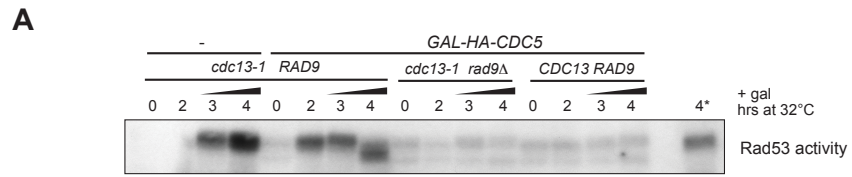
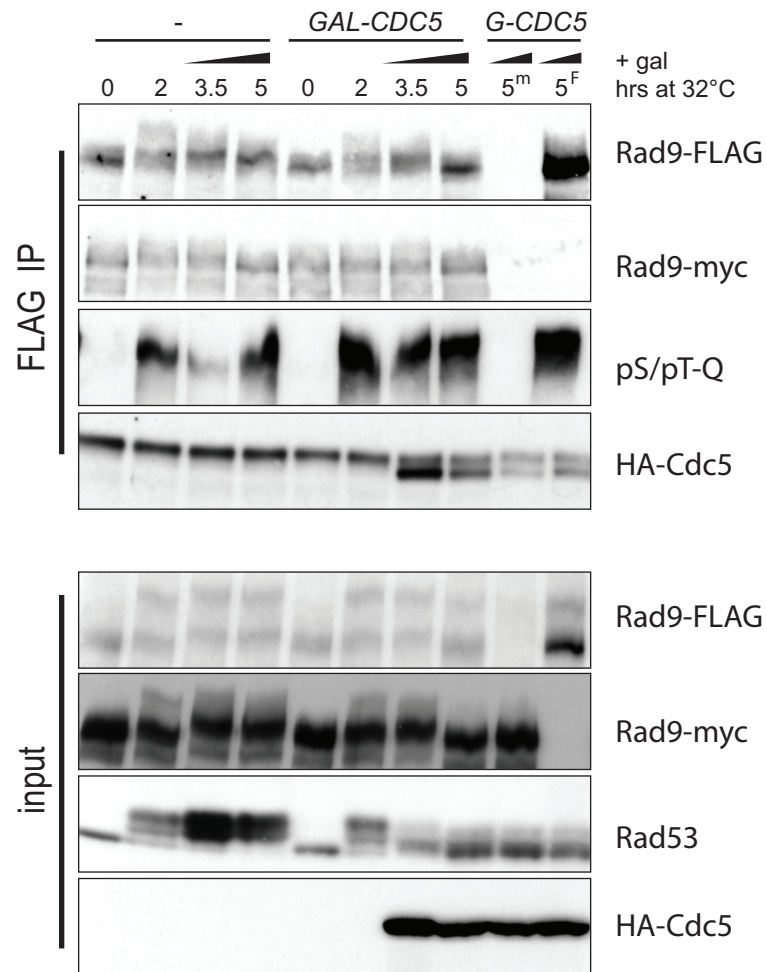


Figure 4. Rad53 interacts with and is phosphorylated by Cdc5 *in vivo* and *in vitro*.

(A) Rad53 was immunoprecipitated from strains shifted to 32°C for 2 hours followed by galactose addition to induce the blank or *HA-CDC5*. As added controls, *rad9Δ* and *CDC13* strains were also analyzed. Rad53 activity was measured by *in situ* kinase assay from the lysates. Asterisk denotes the lane with half the amount of sample as loaded in lane 4. (B) Lysates and IP samples from the experiment described in (A) were analyzed by western blotting by the indicated antibodies. (C and D) *In vitro* kinase assays were performed with purified HA-Cdc5 kinase from (C) undamaged or (D) zeocin treated cells. The substrates were purified recombinant kinase-dead rad53 (D339A, listed as WT) in combination with R70A (FHA1) and/or R605A (FHA2) mutations. (E) *RAD53 cdc5-ad*, *RAD53 CDC5*, *rad53-R70A CDC5* strains were analyzed by adaptation assay. Data shown as percentage of cells per microcolony and as a representative graph of multiple clones.

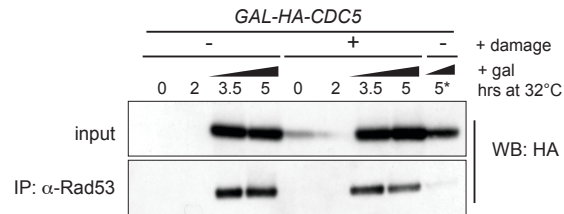


Supplemental Figure 1. Rad9-Rad9 Interaction unaffected by Cdc5. Rad9-FLAG was immunoprecipitated from strains containing a copy of each RAD9-FLAG and RAD9-18myc that were damaged for 2 hours at the non-permissive temperature for *cdc13-1*, then treated with galactose to induce *HA-CDC5*. The 5^m and 5^F denote the 5 hour timepoint of strains that express only RAD9-18myc or RAD9-FLAG, respectively. Input and IP samples were analyzed by western blotting with the indicated antibodies.

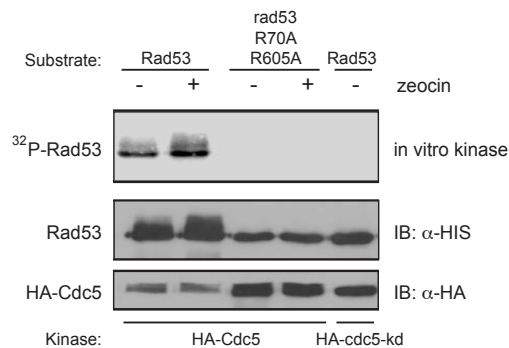


Supplemental Figure 2. Cdc5 and Rad53 interact *in vivo* independently of damage.

Western blot of HA-Cdc5 from input and immunoprecipitated Rad53. Strains listed as -/+ damage are *CDC13* and *cdc13-1*, respectively. Asterisk denotes *rad53Δ*.

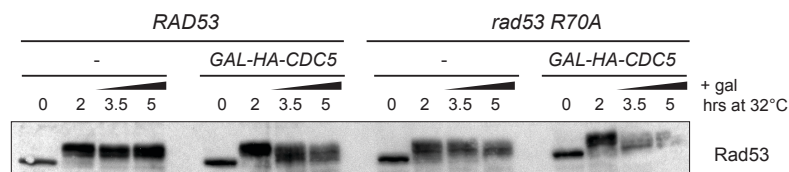


Supplemental Figure 3. Cdc5 phosphorylates Rad53 *in vitro*. *In vitro* kinase assay performed with purified HA-Cdc5 or kinase dead HA-cdc5-K110A from undamaged or zeocin-treated cells. The substrates (all kinase-dead, D339A) were purified recombinant Rad53 or rad53 R70A R605A (FHA double mutant).



Supplemental Figure 4. rad53-R70A hyperphosphorylation is suppressed by Cdc5.

Western blot of Rad53 in *RAD53* or *rad53 R70A* strains that have been damaged and induced for *HA-CDC5* expression.



APPENDIX

TABLE 1. Yeast Strains

Strain Name	Genotype	Created by	Lab
yJK8-1	MAT Δ can1 ade2 trp1 his3 ura3 leu2 lys5 cyh2 ade3::GalHO tel::HO site::ura3::HIS3 Ddc1-GFP::LEU2	J. Kaye	Toczyski
yTMN8H	MAT Δ can1 ade2 trp1 his3 ura3 leu2 lys5 cyh2 ade3::GalHO tel::HO site::ura3::HIS3 RFA3-GFP::KAN	T. Ng	Toczyski
yGMV52-1	MAT Δ can1 ade2 trp1 his3 ura3 leu2 lys5 cyh2 ade3::GalHO tel::HO site::ura3::HIS3 PRI2-GFP::KAN	G. Vidanes	Toczyski
PGY1702	MATa his3 trp1 leu2 ura3 ade2 lys2 DDC2-GFP::KAN	P. Garber	Toczyski
PGY1701	MATa his3 trp1 leu2 ura3 ade2 lys2 DDC2-GFP::KAN rfa1::loxP TRP1::rfa1Y29H	P. Garber	Toczyski
PGY1697	MATa his3 trp1 leu2 ura3 ade2 lys2 DDC1-GFP::LEU2	P. Garber	Toczyski
PGY1696	MATa his3 trp1 leu2 ura3 ade2 lys2 DDC1-GFP::LEU2 rfa1::loxP TRP1::rfa1Y29H	P. Garber	Toczyski
yGMV37a	MAT Δ can1 ade2 trp1 his3 ura3 leu2 lys5 cyh2 ade3::GalHO tel::HO site::ura3::HIS3 Ddc1-GFP::LEU2 URA3::GAL-pol1cd	G. Vidanes	Toczyski
yGMV38a	MAT Δ can1 ade2 trp1 his3 ura3 leu2 lys5 cyh2 ade3::GalHO tel::HO site::ura3::HIS3 Ddc1-GFP::LEU2 URA3::GAL-POL1	G. Vidanes	Toczyski
POL1-GFP	MATa his3 Δ 1 leu2 Δ 0 met15 Δ 0 ura3 Δ 0 POL1-GFP::His3MX		Weissman/ O'Shea
POL12-GFP	MATa his3 Δ 1 leu2 Δ 0 met15 Δ 0 ura3 Δ 0 POL12-GFP::His3MX		Weissman/ O'Shea
NUP170-GFP	MATa his3 Δ 1 leu2 Δ 0 met15 Δ 0 ura3 Δ 0 NUP170-GFP::His3MX		Weissman/ O'Shea
ADR21	MATa his3 trp1 leu2 ura3 ade2 lys2		
PGY1452	MATa his3 trp1 leu2 ura3 ade2 lys2 pri2-1	P. Garber	Toczyski
PGY1460	MATa his3 trp1 leu2 ura3 ade2 lys2 pri2-1 rad24 Δ ::TRP1	P. Garber	Toczyski
PGY1545	MATa his3 trp1 leu2 ura3 ade2 lys2 pri1-M4	P. Garber	Toczyski
PGY1554	MATa his3 trp1 leu2 ura3 ade2 lys2 pri1-M4 rad24 Δ ::TRP1	P. Garber	Toczyski
PGY1575	MATa his3 trp1 leu2 ura3 ade2 lys2 rfa1::loxP TRP1::rfa1Y29H	P. Garber	Toczyski

PGY1579	MATa his3 trp1 leu2 ura3 ade2 lys2 rfa1::loxP TRP1::rfa1Y29H rad17Δ::LEU2	P. Garber	Toczyski
yGMV45-1	MATΔcan1 ade2 trp1 his3 ura3 leu2 lys5 cyh2 ade3::GalHO tel::HO site::ura3::HIS3 DDC1-TAP::URA3	G. Vidanes	Toczyski
yDPB01	MATΔcan1 ade2 trp1 his3 ura3 leu2 lys5 cyh2 ade3::GalHO tel::HO site::ura3::HIS3 DDC2-TAP::URA3	D. Bayless	Toczyski
yGMV65-1*	hoΔ hmlΔ::ADE1 MATa hmrΔ::ADE1 leu2-3,112 lys5, trp1::hisG ura3-52 ade3::GAL10::HO DDC1-TAP::URA3	G. Vidanes	Toczyski
yGMV105-1	(LS) MatΔ cdc13-1 cyh2 can1 lys5 ade2 ade3::GalHO trp1 his3 ura3 leu2 pep4::LEU2 RAD9-FLAG::hyg	G. Vidanes	Toczyski
yGMV106-1	(LS) MatΔ cdc13-1 cyh2 can1 lys5 ade2 ade3::GalHO trp1 his3 ura3 leu2 pep4::LEU2 URA3::GalCDC5-HA(2 copies) RAD9-FLAG::hyg	G. Vidanes	Toczyski
yDPT1-1	(LS) MatΔ cdc13-1 cyh2 can1 lys5 ade2 ade3::GalHO trp1 his3 ura3 leu2 pep4::LEU2	D. Toczyski	Toczyski
yDPT42-4	(LS) MatΔ cdc13-1 cyh2 can1 lys5 ade2 ade3::GalHO trp1 his3 ura3 leu2 pep4::LEU2 URA3::pGAL-HA3-CDC5(2 copies)	D. Toczyski	Toczyski
yGMV110-1	(LS) MatΔ cdc13-1 cyh2 can1 lys5 ade2 ade3::GalHO trp1 his3 ura3 leu2 pep4::LEU2 URA3::pGAL-HA3-cdc5- K110A	G. Vidanes	Toczyski
yGMV111-1	(LS) MatΔ cdc13-1 cyh2 can1 lys5 ade2 ade3::GalHO trp1 his3 ura3 leu2 pep4::LEU2 URA3::pGAL-HA3-cdc5- L251W-HA3	G. Vidanes	Toczyski
yGMV155	(LS) MatΔ cdc13-1 cyh2 can1 lys5 ade2 ade3::GalHO trp1 his3 ura3 leu2 pep4::LEU2 RAD9-FLAG::HYG ptc3Δ::TRP1 ptc2Δ::KAN	G. Vidanes	Toczyski
yGMV156-1	(LS) MatΔ cdc13-1 cyh2 can1 lys5 ade2 ade3::GalHO trp1 his3 ura3 leu2 pep4::LEU2 RAD9-FLAG::HYG ptc3Δ::TRP1 ptc2Δ::KAN GAL-3HA- CDC5-URA3::CDC5	G. Vidanes	Toczyski
yGMV175-1	(LS) MatΔ cdc13-1 cyh2 can1 lys5 ade2 ade3::GalHO trp1 his3 ura3 leu2 pep4::LEU2 rad9Δ::hyg	G. Vidanes	Toczyski
yGMV177-1	(LS) MatΔ cdc13-1 cyh2 can1 lys5 ade2 ade3::GalHO trp1 his3 ura3 leu2 pep4::LEU2 URA3::pGAL-HA3-CDC5(2 copies) rad9Δ::hyg	G. Vidanes	Toczyski

yGMV184-3	(LS) MatΔ cdc13-1 cyh2 can1 lys5 ade2 ade3::GalHO trp1 his3 ura3 leu2 pep4::LEU2 RAD9-FLAG::hyg URA3::GAL-CDC14-Pk	G. Vidanes	Toczyski
yGMV185-2	(LS) MatΔ cdc13-1 cyh2 can1 lys5 ade2 ade3::GalHO trp1 his3 ura3 leu2 pep4::LEU2 RAD9-FLAG::HYG CDC13::TRP1 URA3::GAL-CDC14-Pk	G. Vidanes	Toczyski
yGMV144-1	(LS) MatΔ cdc13-1 cyh2 can1 lys5 ade2 ade3::GalHO trp1 his3 ura3 leu2 pep4::LEU2 RAD9-FLAG::HYG CDC13::TRP1	G. Vidanes	Toczyski
yGMV145-1	(LS) MatΔ cdc13-1 cyh2 can1 lys5 ade2 ade3::GalHO trp1 his3 ura3 leu2 pep4::LEU2 URA3::GalCDC5-HA(2 copies) RAD9-FLAG::HYG CDC13::TRP1	G. Vidanes	Toczyski
yGMV168-1	(LS) MatΔ cdc13-1 cyh2 can1 lys5 ade2 ade3::GalHO trp1 his3 ura3 leu2 pep4::LEU2 RAD53::TRP1	G. Vidanes	Toczyski
yGMV169-1	(LS) MatΔ cdc13-1 cyh2 can1 lys5 ade2 ade3::GalHO trp1 his3 ura3 leu2 pep4::LEU2 rad53-R70A::TRP1	G. Vidanes	Toczyski
yGMV170-1	(LS) MatΔ cdc13-1 cyh2 can1 lys5 ade2 ade3::GalHO trp1 his3 ura3 leu2 pep4::LEU2 URA3::GalCDC5-HA(2 copies) RAD53::TRP1	G. Vidanes	Toczyski
yGMV171-1	(LS) MatΔ cdc13-1 cyh2 can1 lys5 ade2 ade3::GalHO trp1 his3 ura3 leu2 pep4::LEU2 URA3::GalCDC5-HA(2 copies) rad53-R70A::TRP1	G. Vidanes	Toczyski
yDPT2-1	MatΔ cdc13-1 cyh2 can1 lys5 ade2 ade3::GalHO trp1 his3 ura3 leu2 pep4::LEU2 cdc5-ad	D. Toczyski	Toczyski
yGMV186	(LS) MatΔ cdc13-1 cyh2 can1 lys5 ade2 ade3::GalHO trp1 his3 ura3 leu2 pep4::LEU2 RAD9-myc::TRP1	G. Vidanes	Toczyski
yGMV187	(LS) MatΔ cdc13-1 cyh2 can1 lys5 ade2 ade3::GalHO trp1 his3 ura3 leu2 pep4::LEU2 URA3::pGAL-HA3-CDC5(2 copies) RAD9-myc::TRP1	G. Vidanes	Toczyski
yGMV188-1	(LS) MatΔ cdc13-1 cyh2 can1 lys5 ade2 ade3::GalHO trp1 his3 ura3 leu2 pep4::LEU2 RAD9-FLAG::hyg RAD9- myc::TRP1	G. Vidanes	Toczyski
yGMV189	(LS) MatΔ cdc13-1 cyh2 can1 lys5 ade2 ade3::GalHO trp1 his3 ura3 leu2 pep4::LEU2 URA3::GalCDC5-HA(2 copies) RAD9-FLAG::hyg RAD9- myc::TRP1	G. Vidanes	Toczyski

*The parent strain, yJKM139, was a kind gift from J. Haber.

BIBLIOGRAPHY

1. Melo J, Toczyski D (2002) A unified view of the DNA-damage checkpoint. *Curr Opin Cell Biol* 14: 237-245.
2. Kondo T, Wakayama T, Naiki T, Matsumoto K, Sugimoto K (2001) Recruitment of *mec1* and *ddc1* checkpoint proteins to double-strand breaks through distinct mechanisms. *Science* 294: 867-870.
3. Melo JA, Cohen J, Toczyski DP (2001) Two checkpoint complexes are independently recruited to sites of DNA damage in vivo. *Genes Dev* 15: 2809-2821.
4. Zou L, Liu D, Elledge SJ (2003) Replication protein A-mediated recruitment and activation of Rad17 complexes. *Proc Natl Acad Sci U S A* 100: 13827-13832.
5. Zou L, Elledge SJ (2003) Sensing DNA damage through ATRIP recognition of RPA-ssDNA complexes. *Science* 300: 1542-1548.
6. Nakada D, Matsumoto K, Sugimoto K (2003) ATM-related Tel1 associates with double-strand breaks through an Xrs2-dependent mechanism. *Genes Dev* 17: 1957-1962.
7. van den Bosch M, Bree RT, Lowndes NF (2003) The MRN complex: coordinating and mediating the response to broken chromosomes. *EMBO Rep* 4: 844-849.
8. Weterings E, van Gent DC (2004) The mechanism of non-homologous end-joining: a synopsis of synapsis. *DNA Repair (Amst)* 3: 1425-1435.
9. Krogh BO, Symington LS (2004) Recombination Proteins in Yeast. *Annu Rev Genet.*
10. Wolner B, van Komen S, Sung P, Peterson CL (2003) Recruitment of the recombinational repair machinery to a DNA double-strand break in yeast. *Mol Cell* 12: 221-232.

11. Sugawara N, Wang X, Haber JE (2003) In vivo roles of Rad52, Rad54, and Rad55 proteins in Rad51-mediated recombination. *Mol Cell* 12: 209-219.
12. Frank-Vaillant M, Marcand S (2002) Transient stability of DNA ends allows nonhomologous end joining to precede homologous recombination. *Mol Cell* 10: 1189-1199.
13. Lee SE, Moore JK, Holmes A, Umezumi K, Kolodner RD, et al. (1998) *Saccharomyces* Ku70, mre11/rad50 and RPA proteins regulate adaptation to G2/M arrest after DNA damage. *Cell* 94: 399-409.
14. Lisby M, Barlow JH, Burgess RC, Rothstein R (2004) Choreography of the DNA damage response: spatiotemporal relationships among checkpoint and repair proteins. *Cell* 118: 699-713.
15. Ira G, Pellicoli A, Balijja A, Wang X, Fiorani S, et al. (2004) DNA end resection, homologous recombination and DNA damage checkpoint activation require CDK1. *Nature* 431: 1011-1017.
16. Ubersax JA, Woodbury EL, Quang PN, Paraz M, Blethrow JD, et al. (2003) Targets of the cyclin-dependent kinase Cdk1. *Nature* 425: 859-864.
17. Usui T, Ogawa H, Petrini JH (2001) A DNA damage response pathway controlled by Tel1 and the Mre11 complex. *Mol Cell* 7: 1255-1266.
18. Shroff R, Arbel-Eden A, Pilch D, Ira G, Bonner WM, et al. (2004) Distribution and dynamics of chromatin modification induced by a defined DNA double-strand break. *Curr Biol* 14: 1703-1711.

19. Siede W, Friedl AA, Dianova I, Eckardt-Schupp F, Friedberg EC (1996) The *Saccharomyces cerevisiae* Ku autoantigen homologue affects radiosensitivity only in the absence of homologous recombination. *Genetics* 142: 91-102.
20. Khanna KK, Jackson SP (2001) DNA double-strand breaks: signaling, repair and the cancer connection. *Nat Genet* 27: 247-254.
21. Kurz EU, Lees-Miller SP (2004) DNA damage-induced activation of ATM and ATM-dependent signaling pathways. *DNA Repair (Amst)* 3: 889-900.
22. Fukushima T, Takata M, Morrison C, Araki R, Fujimori A, et al. (2001) Genetic analysis of the DNA-dependent protein kinase reveals an inhibitory role of Ku in late S-G2 phase DNA double-strand break repair. *J Biol Chem* 276: 44413-44418.
23. Burma S, Chen DJ (2004) Role of DNA-PK in the cellular response to DNA double-strand breaks. *DNA Repair (Amst)* 3: 909-918.
24. Nelms BE, Maser RS, MacKay JF, Lagally MG, Petrini JH (1998) In situ visualization of DNA double-strand break repair in human fibroblasts. *Science* 280: 590-592.
25. Maser RS, Monsen KJ, Nelms BE, Petrini JH (1997) hMre11 and hRad50 nuclear foci are induced during the normal cellular response to DNA double-strand breaks. *Mol Cell Biol* 17: 6087-6096.
26. Takata M, Sasaki MS, Sonoda E, Morrison C, Hashimoto M, et al. (1998) Homologous recombination and non-homologous end-joining pathways of DNA double-strand break repair have overlapping roles in the maintenance of chromosomal integrity in vertebrate cells. *Embo J* 17: 5497-5508.
27. Kamakaka RT, Biggins S (2005) Histone variants: deviants? *Genes Dev* 19: 295-310.

28. Pilch DR, Sedelnikova OA, Redon C, Celeste A, Nussenzweig A, et al. (2003) Characteristics of gamma-H2AX foci at DNA double-strand breaks sites. *Biochem Cell Biol* 81: 123-129.
29. Celeste A, Fernandez-Capetillo O, Kruhlak MJ, Pilch DR, Staudt DW, et al. (2003) Histone H2AX phosphorylation is dispensable for the initial recognition of DNA breaks. *Nat Cell Biol* 5: 675-679.
30. Celeste A, Petersen S, Romanienko PJ, Fernandez-Capetillo O, Chen HT, et al. (2002) Genomic instability in mice lacking histone H2AX. *Science* 296: 922-927.
31. Downs JA, Allard S, Jobin-Robitaille O, Javaheri A, Auger A, et al. (2004) Binding of chromatin-modifying activities to phosphorylated histone H2A at DNA damage sites. *Mol Cell* 16: 979-990.
32. Unal E, Arbel-Eden A, Sattler U, Shroff R, Lichten M, et al. (2004) DNA damage response pathway uses histone modification to assemble a double-strand break-specific cohesin domain. *Mol Cell* 16: 991-1002.
33. van Attikum H, Fritsch O, Hohn B, Gasser SM (2004) Recruitment of the INO80 complex by H2A phosphorylation links ATP-dependent chromatin remodeling with DNA double-strand break repair. *Cell* 119: 777-788.
34. Downs JA, Lowndes NF, Jackson SP (2000) A role for *Saccharomyces cerevisiae* histone H2A in DNA repair. *Nature* 408: 1001-1004.
35. Nakamura TM, Du LL, Redon C, Russell P (2004) Histone H2A phosphorylation controls Crb2 recruitment at DNA breaks, maintains checkpoint arrest, and influences DNA repair in fission yeast. *Mol Cell Biol* 24: 6215-6230.

36. Kobayashi J, Tauchi H, Sakamoto S, Nakamura A, Morishima K, et al. (2002) NBS1 localizes to gamma-H2AX foci through interaction with the FHA/BRCT domain. *Curr Biol* 12: 1846-1851.
37. Strom L, Lindroos HB, Shirahige K, Sjogren C (2004) Postreplicative recruitment of cohesin to double-strand breaks is required for DNA repair. *Mol Cell* 16: 1003-1015.
38. Ward IM, Minn K, Jorda KG, Chen J (2003) Accumulation of checkpoint protein 53BP1 at DNA breaks involves its binding to phosphorylated histone H2AX. *J Biol Chem* 278: 19579-19582.
39. Morrison AJ, Highland J, Krogan NJ, Arbel-Eden A, Greenblatt JF, et al. (2004) INO80 and gamma-H2AX interaction links ATP-dependent chromatin remodeling to DNA damage repair. *Cell* 119: 767-775.
40. Bird AW, Yu DY, Pray-Grant MG, Qiu Q, Harmon KE, et al. (2002) Acetylation of histone H4 by Esa1 is required for DNA double-strand break repair. *Nature* 419: 411-415.
41. Ehrenhofer-Murray AE (2004) Chromatin dynamics at DNA replication, transcription and repair. *Eur J Biochem* 271: 2335-2349.
42. Kusch T, Florens L, Macdonald WH, Swanson SK, Glaser RL, et al. (2004) Acetylation by Tip60 is required for selective histone variant exchange at DNA lesions. *Science* 306: 2084-2087.
43. Huyen Y, Zgheib O, Ditullio RA, Jr., Gorgoulis VG, Zacharatos P, et al. (2004) Methylated lysine 79 of histone H3 targets 53BP1 to DNA double-strand breaks. *Nature* 432: 406-411.

44. Giannattasio M, Lazzaro F, Plevani P, Muzi-Falconi M (2005) The DNA damage checkpoint response requires histone H2B ubiquitination by Rad6-Bre1 and H3 methylation by Dot1. *J Biol Chem* 280: 9879-9886.
45. Sanders SL, Portoso M, Mata J, Bahler J, Allshire RC, et al. (2004) Methylation of histone H4 lysine 20 controls recruitment of Crb2 to sites of DNA damage. *Cell* 119: 603-614.
46. van Leeuwen F, Gafken PR, Gottschling DE (2002) Dot1p modulates silencing in yeast by methylation of the nucleosome core. *Cell* 109: 745-756.
47. Ng HH, Ciccone DN, Morshead KB, Oettinger MA, Struhl K (2003) Lysine-79 of histone H3 is hypomethylated at silenced loci in yeast and mammalian cells: a potential mechanism for position-effect variegation. *Proc Natl Acad Sci U S A* 100: 1820-1825.
48. Lydall D, Weinert T (1995) Yeast checkpoint genes in DNA damage processing: implications for repair and arrest. *Science* 270: 1488-1491.
49. Yuzhakov A, Kelman Z, Hurwitz J, O'Donnell M (1999) Multiple competition reactions for RPA order the assembly of the DNA polymerase delta holoenzyme. *Embo J* 18: 6189-6199.
50. Venclovas C, Thelen MP (2000) Structure-based predictions of Rad1, Rad9, Hus1 and Rad17 participation in sliding clamp and clamp-loading complexes. *Nucleic Acids Res* 28: 2481-2493.
51. Majka J, Burgers PM (2003) Yeast Rad17/Mec3/Ddc1: a sliding clamp for the DNA damage checkpoint. *Proc Natl Acad Sci U S A* 100: 2249-2254.

52. Ellison V, Stillman B (2003) The PCNA and Rad9-Hus1-Rad1 Complex Form Sliding Clamps on Distinct DNA Structures. CSHL Eukaryotic DNA Replication abstract book: 124.
53. Bermudez VP, Lindsey-Boltz LA, Cesare AJ, Maniwa Y, Griffith JD, et al. (2003) Loading of the human 9-1-1 checkpoint complex onto DNA by the checkpoint clamp loader hRad17-replication factor C complex in vitro. Proc Natl Acad Sci U S A 100: 1633-1638.
54. Sundin BA, Chiu CH, Riffle M, Davis TN, Muller EG (2004) Localization of proteins that are coordinately expressed with Cln2 during the cell cycle. Yeast 21: 793-800.
55. Rouse J, Jackson SP (2000) LCD1: an essential gene involved in checkpoint control and regulation of the MEC1 signalling pathway in *Saccharomyces cerevisiae*. Embo J 19: 5801-5812.
56. Longhese MP, Paciotti V, Fraschini R, Zaccarini R, Plevani P, et al. (1997) The novel DNA damage checkpoint protein ddc1p is phosphorylated periodically during the cell cycle and in response to DNA damage in budding yeast. Embo J 16: 5216-5226.
57. Foiani M, Liberi G, Lucchini G, Plevani P (1995) Cell cycle-dependent phosphorylation and dephosphorylation of the yeast DNA polymerase alpha-primase B subunit. Mol Cell Biol 15: 883-891.
58. Nguyen VQ, Co C, Li JJ (2001) Cyclin-dependent kinases prevent DNA re-replication through multiple mechanisms. Nature 411: 1068-1073.

59. Heun P, Laroche T, Raghuraman MK, Gasser SM (2001) The positioning and dynamics of origins of replication in the budding yeast nucleus. *J Cell Biol* 152: 385-400.
60. Raghuraman MK, Winzeler EA, Collingwood D, Hunt S, Wodicka L, et al. (2001) Replication dynamics of the yeast genome. *Science* 294: 115-121.
61. Desdouets C, Santocanale C, Drury LS, Perkins G, Foiani M, et al. (1998) Evidence for a Cdc6p-independent mitotic resetting event involving DNA polymerase alpha. *Embo J* 17: 4139-4146.
62. Sugawara N, Haber JE (1992) Characterization of double-strand break-induced recombination: homology requirements and single-stranded DNA formation. *Mol Cell Biol* 12: 563-575.
63. Garvik B, Carson M, Hartwell L (1995) Single-stranded DNA arising at telomeres in *cdc13* mutants may constitute a specific signal for the RAD9 checkpoint. *Mol Cell Biol* 15: 6128-6138.
64. Ellison V, Stillman B (2003) Biochemical characterization of DNA damage checkpoint complexes: clamp loader and clamp complexes with specificity for 5' recessed DNA. *PLoS Biol* 1: E33.
65. Sanchez Y, Desany BA, Jones WJ, Liu Q, Wang B, et al. (1996) Regulation of RAD53 by the ATM-like kinases MEC1 and TEL1 in yeast cell cycle checkpoint pathways. *Science* 271: 357-360.
66. Bonilla CY, Melo JA, Toczyski DP (2008) Colocalization of sensors is sufficient to activate the DNA damage checkpoint in the absence of damage. *Mol Cell* 30: 267-276.

67. Lee SJ, Duong JK, Stern DF (2004) A Ddc2-Rad53 fusion protein can bypass the requirements for RAD9 and MRC1 in Rad53 activation. *Mol Biol Cell* 15: 5443-5455.
68. Alcasabas AA, Osborn AJ, Bachant J, Hu F, Werler PJ, et al. (2001) Mrc1 transduces signals of DNA replication stress to activate Rad53. *Nat Cell Biol* 3: 958-965.
69. Emili A (1998) MEC1-dependent phosphorylation of Rad9p in response to DNA damage. *Mol Cell* 2: 183-189.
70. Sun Z, Hsiao J, Fay DS, Stern DF (1998) Rad53 FHA domain associated with phosphorylated Rad9 in the DNA damage checkpoint. *Science* 281: 272-274.
71. Sanchez Y, Bachant J, Wang H, Hu F, Liu D, et al. (1999) Control of the DNA damage checkpoint by chk1 and rad53 protein kinases through distinct mechanisms. *Science* 286: 1166-1171.
72. Blankley RT, Lydall D (2004) A domain of Rad9 specifically required for activation of Chk1 in budding yeast. *J Cell Sci* 117: 601-608.
73. Sweeney FD, Yang F, Chi A, Shabanowitz J, Hunt DF, et al. (2005) *Saccharomyces cerevisiae* Rad9 acts as a Mec1 adaptor to allow Rad53 activation. *Curr Biol* 15: 1364-1375.
74. Vialard JE, Gilbert CS, Green CM, Lowndes NF (1998) The budding yeast Rad9 checkpoint protein is subjected to Mec1/Tel1-dependent hyperphosphorylation and interacts with Rad53 after DNA damage. *EMBO J* 17: 5679-5688.
75. Xu YJ, Davenport M, Kelly TJ (2006) Two-stage mechanism for activation of the DNA replication checkpoint kinase Cds1 in fission yeast. *Genes Dev* 20: 990-1003.

76. Toczyski DP, Galgoczy DJ, Hartwell LH (1997) CDC5 and CKII control adaptation to the yeast DNA damage checkpoint. *Cell* 90: 1097-1106.
77. Pellicioli A, Lee SE, Lucca C, Foiani M, Haber JE (2001) Regulation of *Saccharomyces* Rad53 checkpoint kinase during adaptation from DNA damage-induced G2/M arrest. *Mol Cell* 7: 293-300.
78. Yoo HY, Kumagai A, Shevchenko A, Dunphy WG (2004) Adaptation of a DNA replication checkpoint response depends upon inactivation of Claspin by the Polo-like kinase. *Cell* 117: 575-588.
79. Mailand N, Bekker-Jensen S, Bartek J, Lukas J (2006) Destruction of Claspin by SCFbetaTrCP restrains Chk1 activation and facilitates recovery from genotoxic stress. *Mol Cell* 23: 307-318.
80. Peschiaroli A, Dorrello NV, Guardavaccaro D, Venere M, Halazonetis T, et al. (2006) SCFbetaTrCP-mediated degradation of Claspin regulates recovery from the DNA replication checkpoint response. *Mol Cell* 23: 319-329.
81. Mamely I, van Vugt MA, Smits VA, Semple JI, Lemmens B, et al. (2006) Polo-like kinase-1 controls proteasome-dependent degradation of Claspin during checkpoint recovery. *Curr Biol* 16: 1950-1955.
82. Toczyski DP (2006) Methods for studying adaptation to the DNA damage checkpoint in yeast. *Methods Enzymol* 409: 150-165.
83. Leroy C, Lee SE, Vaze MB, Ochsenbien F, Guerois R, et al. (2003) PP2C phosphatases Ptc2 and Ptc3 are required for DNA checkpoint inactivation after a double-strand break. *Mol Cell* 11: 827-835.

84. Guillemain G, Ma E, Mauger S, Miron S, Thai R, et al. (2007) Mechanisms of checkpoint kinase Rad53 inactivation after a double-strand break in *Saccharomyces cerevisiae*. *Mol Cell Biol* 27: 3378-3389.
85. Visintin R, Stegmeier F, Amon A (2003) The role of the polo kinase Cdc5 in controlling Cdc14 localization. *Mol Biol Cell* 14: 4486-4498.
86. Clerici M, Baldo V, Mantiero D, Lotterberger F, Lucchini G, et al. (2004) A Tel1/MRX-dependent checkpoint inhibits the metaphase-to-anaphase transition after UV irradiation in the absence of Mec1. *Mol Cell Biol* 24: 10126-10144.
87. Jazayeri A, Falck J, Lukas C, Bartek J, Smith GC, et al. (2006) ATM- and cell cycle-dependent regulation of ATR in response to DNA double-strand breaks. *Nat Cell Biol* 8: 37-45.
88. Pelliccioli A, Lucca C, Liberi G, Marini F, Lopes M, et al. (1999) Activation of Rad53 kinase in response to DNA damage and its effect in modulating phosphorylation of the lagging strand DNA polymerase. *EMBO J* 18: 6561-6572.
89. Elia AE, Rellos P, Haire LF, Chao JW, Ivins FJ, et al. (2003) The molecular basis for phosphodependent substrate targeting and regulation of Plks by the Polo-box domain. *Cell* 115: 83-95.
90. Sun Z, Fay DS, Marini F, Foiani M, Stern DF (1996) Spk1/Rad53 is regulated by Mec1-dependent protein phosphorylation in DNA replication and damage checkpoint pathways. *Genes Dev* 10: 395-406.
91. Durocher D, Henckel J, Fersht AR, Jackson SP (1999) The FHA domain is a modular phosphopeptide recognition motif. *Mol Cell* 4: 387-394.

92. Tsvetkov L, Xu X, Li J, Stern DF (2003) Polo-like kinase 1 and Chk2 interact and co-localize to centrosomes and the midbody. *J Biol Chem* 278: 8468-8475.
93. Tsvetkov LM, Tsekova RT, Xu X, Stern DF (2005) The Plk1 Polo box domain mediates a cell cycle and DNA damage regulated interaction with Chk2. *Cell Cycle* 4: 609-617.
94. Pike BL, Yongkiettrakul S, Tsai MD, Heierhorst J (2003) Diverse but overlapping functions of the two forkhead-associated (FHA) domains in Rad53 checkpoint kinase activation. *J Biol Chem* 278: 30421-30424.
95. Durocher D, Taylor IA, Sarbassova D, Haire LF, Westcott SL, et al. (2000) The molecular basis of FHA domain:phosphopeptide binding specificity and implications for phospho-dependent signaling mechanisms. *Mol Cell* 6: 1169-1182.
96. Mortensen EM, Haas W, Gygi M, Gygi SP, Kellogg DR (2005) Cdc28-dependent regulation of the Cdc5/Polo kinase. *Curr Biol* 15: 2033-2037.
97. Charles JF, Jaspersen SL, Tinker-Kulberg RL, Hwang L, Szidon A, et al. (1998) The Polo-related kinase Cdc5 activates and is destroyed by the mitotic cyclin destruction machinery in *S. cerevisiae*. *Curr Biol* 8: 497-507.
98. Petronczki M, Lenart P, Peters JM (2008) Polo on the Rise-from Mitotic Entry to Cytokinesis with Plk1. *Dev Cell* 14: 646-659.
99. Alexandru G, Uhlmann F, Mechtler K, Poupart MA, Nasmyth K (2001) Phosphorylation of the cohesin subunit Scc1 by Polo/Cdc5 kinase regulates sister chromatid separation in yeast. *Cell* 105: 459-472.

100. Barr FA, Sillje HH, Nigg EA (2004) Polo-like kinases and the orchestration of cell division. *Nat Rev Mol Cell Biol* 5: 429-440.
101. Usui T, Foster SS, Petrini JH (2009) Maintenance of the DNA-damage checkpoint requires DNA-damage-induced mediator protein oligomerization. *Mol Cell* 33: 147-159.
102. Gilbert CS, Green CM, Lowndes NF (2001) Budding yeast Rad9 is an ATP-dependent Rad53 activating machine. *Mol Cell* 8: 129-136.
103. Lowery DM, Mohammad DH, Elia AE, Yaffe MB (2004) The Polo-box domain: a molecular integrator of mitotic kinase cascades and Polo-like kinase function. *Cell Cycle* 3: 128-131.
104. Schwartz MF, Lee SJ, Duong JK, Eminaga S, Stern DF (2003) FHA domain-mediated DNA checkpoint regulation of Rad53. *Cell Cycle* 2: 384-396.
105. Liao H, Yuan C, Su MI, Yongkiettrakul S, Qin D, et al. (2000) Structure of the FHA1 domain of yeast Rad53 and identification of binding sites for both FHA1 and its target protein Rad9. *J Mol Biol* 304: 941-951.
106. Liao H, Byeon IJ, Tsai MD (1999) Structure and function of a new phosphopeptide-binding domain containing the FHA2 of Rad53. *J Mol Biol* 294: 1041-1049.
107. Pike BL, Yongkiettrakul S, Tsai MD, Heierhorst J (2004) Mdt1, a novel Rad53 FHA1 domain-interacting protein, modulates DNA damage tolerance and G(2)/M cell cycle progression in *Saccharomyces cerevisiae*. *Mol Cell Biol* 24: 2779-2788.
108. Duncker BP, Shimada K, Tsai-Pflugfelder M, Pasero P, Gasser SM (2002) An N-terminal domain of Dbf4p mediates interaction with both origin recognition

complex (ORC) and Rad53p and can deregulate late origin firing. Proc Natl Acad Sci U S A 99: 16087-16092.

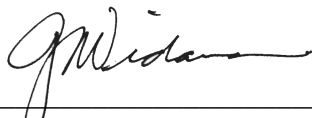
109. Galgoczy DJ, Toczyski DP (2001) Checkpoint adaptation precedes spontaneous and damage-induced genomic instability in yeast. Mol Cell Biol 21: 1710-1718.
110. Takai N, Hamanaka R, Yoshimatsu J, Miyakawa I (2005) Polo-like kinases (Plks) and cancer. Oncogene 24: 287-291.
111. Strebhardt K, Ullrich A (2006) Targeting polo-like kinase 1 for cancer therapy. Nat Rev Cancer 6: 321-330.

Publishing Agreement

It is the policy of the University to encourage the distribution of all theses and dissertations. Copies of all UCSF theses and dissertations will be routed to the library via the Graduate Division. The library will make all theses and dissertations accessible to the public and will preserve these to the best of their abilities, in perpetuity.

Please sign the following statement:

I hereby grant permission to the Graduate Division of the University of California, San Francisco to release copies of my thesis or dissertation to the Campus Library to provide access and preservation, in whole or in part, in perpetuity.



Author Signature

March 26, 2009

Date